A Space-Time Analysis of LTE and Wi-Fi Inter-working

Youjia Chen, Ming Ding, *Member, IEEE*, David López-Pérez, *Member, IEEE*, Zihuai Lin, *Senior Member, IEEE*, and Guoqiang Mao, *Senior Member, IEEE*

***Abstract*—Cooperative inter-working of the Long Term Evolution (LTE) and the Wireless Fidelity (Wi-Fi) networks have drawn much attention recently, and several strategies have been proposed to enhance their network capacity. In this paper, we propose a new framework to analyse the network performance of several inter-working strategies for the LTE and the Wi-Fi. The proposed framework considers both the LTE and the Wi-Fi systems, both the downlink (DL) and the uplink (UL) transmissions, and the generated interference in both the time and the spatial domains. Based on such framework, we theoretically analyse for the first time the performance of a Wi-Fi network, taking into account the intra-cell time efficiency, and the signal and inter-cell interference with spatial randomness. Moreover, we study the performance of *i)* a coexisting architecture where Wi-Fi coexists with an ideal CSMA duplex (ID-CSMA) system, which represents an upper bound performance for the LTE Release 14 licensed assisted access (LAA) network, and *ii)* a brand-new architecture that allows UL on LTE and DL on Wi-Fi, referred to as the *Boost* architecture. We derive analytical results for both the DL and the UL network performance in terms of the signal quality distribution and the total area system throughput (AST) in these two architectures, and quantify their performance gain compared with the traditional disjoint LTE Wi-Fi architecture. Simulation results validate our analysis results, and show that in a typical outdoor scenario, the coexisting architecture and the *Boost* architecture can respectively increase the total AST up to 11% and 25%, compared with the traditional disjoint LTE Wi-Fi.**

I. Introduction

The use of unlicensed spectrum by mobile network operators, particularly in the 5 GHz band, has recently been attracting considerable attention, and vendors and operators are already actively studying its viability for long term evolution (LTE)/4G cellular networks [1]. The use of the unlicensed spectrum for cellular operation represents a significant change in cellular network deployment and management, and there are, at this stage, still many open questions in terms of both business case and technology as a whole.

A major aspect of ongoing discussions is the requirement to provide fair co-existence between this new unlicensed LTE technology and other technologies working in the unlicensed spectrum. Given that current technologies in unlicensed bands, such as Wireless Fidelity (Wi-Fi) [2], rely on contention-based access, there is a concern that starvation and other forms of unfairness may occur when they co-exist with a schedule-based technology such as LTE [3, 4]. Co-existence of multiple LTE operators within the same unlicensed band is also a major concern.

A. The Related 3GPP Standardisation

Two major approaches are being considered within the Third Generation Partnership Project (3GPP) to address this issue, where the main difference between them both is that one uses LTE radio access technology to operate the unlicensed spectrum, while the other accesses it through IEEE 802.11 standards.

The first approach aims at using LTE infrastructure to access the unlicensed band, and thus calls for a harmonious coexistence of this new LTE deployments with the existing Wi-Fi networks in the unlicensed spectrum. The Licensed-assisted access (LAA) [5] technology can be classified within this category, where listen-before-talk (LBT) is the technique used to reinforce co-existence and conform with, for instance, European and Japanese regulations. It is important to note that the LBT used by LAA is similar to the carrier sense multiple access/collision avoidance (CSMA/CA)[1] medium access control (MAC) used by Wi-Fi. A significant advantage of using a similar random access procedure to Wi-Fi devices to win transmission opportunities is that fair co-existence with them can be more easily guaranteed. Importantly, co-existence of multiple LTE networks within the unlicensed band can also be ensured in a more straightforward manner.

The second approach aims at leveraging Wi-Fi infrastructure to access the unlicensed spectrum. Thus, it does not attempt to deploy LTE infrastructure in the unlicensed band but instead seeks to enhance Wi-Fi performance through inter-working techniques.LTE-WLAN Aggregation (LWA) and LTE WLAN Radio Level Integration with IPsec Tunnel (LWIP) [6–8] are examples of this category, where a tight integration of LTE and Wi-Fi allows enhanced performance and quality of service

[1]An overview of CSMA/CA is provided in Appendix A

Youjia Chen is with the School of Electrical and Information Engineering, The University of Sydney, Australia, with Fujian Normal University, China, and also with Data61, CSIRO, Australia. E-mail: youjia.chen@sydney.edu.au.

Ming Ding is with Data61, CSIRO, Australia. E-mail: Ming.Ding@data61.csiro.au.

David López-Pérez is with Bell Laboratories, Nokia, Ireland. E-mail: dr.david.lopez@ieee.org.

Zihuai Lin is with the School of Electrical and Information Engineering, The University of Sydney, Australia, and also with Data61, CSIRO, Australia. E-mail: zihuai.lin@sydney.edu.au.

Guoqiang Mao is with the School of Computing and Communications, The University of Technology Sydney, Australia, and also with Data61, CSIRO, Australia. E-mail: g.mao@ieee.org.

This work is supported by the Fujian Provincial Natural Science Foundation (No. 2016J01290), the National Natural Science Foundation of China (No. 61571128) and the China Scholarship Council.

provisioning. In contrast to LAA, since LWA and LWIP technologies access the unlicensed technology through certified Wi-Fi technology, co-existence and regulatory requirements are not a concern for them.

B. Related Work

In order to obtain a deeper understanding of different mentioned LTE and Wi-Fi cooperation strategies, a new framework is needed to theoretically analyse the network performance considering the features of both LTE and Wi-Fi.

Stochastic geometry has recently become a popular and powerful mathematical tool to analyse large-scale wireless networks. In more detail, by modelling the locations of base stations (BSs) and/or access points (APs) and/or UEs as spatially random point process, several key network performance metrics can be derived.

The performance of LTE has been well analysed using the stochastic geometry theory. In [9–11], the coverage probability and average network capacity were derived for the DL and UL of cellular networks with BSs following the homogeneous Poisson Point Process (HPPP).

In contrast, the performance analysis for Wi-Fi mainly consists of two aspects:

- The Time-Domain Analysis: Regarding the time-domain analysis of Wi-Fi, in [12], the authors proposed a two-dimensional (2-D) Markov chain model to analyse the system utility of a stand-alone Wi-Fi system under the assumption of ideal channel conditions and a finite number of saturated terminals. Such 2-D model was extended in various ways to consider non-saturated traffic, infinite buffer and buffer-less cases, different QoS parameters, etc. [13–15]. However, all of these works were limited to a stand-alone, single cell Wi-Fi system. In practice, the interaction among adjacent Wi-Fi systems in the spatial-domain should be considered, especially for dense Wi-Fi networks.
- The Spatial-Domain Analysis: Regarding the spatial-domain analysis of Wi-Fi, in [16], the authors proposed the use of a modified Matérn hard-core point process (MHCP) to analyse a dense Wi-Fi network, which investigates a snapshot of nodes that can transmit simultaneously according to the CSMA/CA protocol. However, it did not capture the time-domain features of Wi-Fi such as colliding transmissions, exponential back-off and so on, which have a large impact in Wi-Fi systems. The same issue exists in recent works, which analyze the performance of LAA networks [4, 17]. Moreover, all of these existing works focused on the DL transmissions only, and did not treat the UL transmissions, which are the main source of Wi-Fi performance degradation due to intra-cell channel contentions [17].

C. Contributions

The contributions of this paper are four-fold:

- We introduce a new network performance analysis for Wi-Fi networks that simultaneously considers the DL and UL transmissions and jointly investigates *1)* the intra-cell time efficiency degradation caused by the random back-off scheme and transmission collisions, *2)* the signal and inter-cell interference with the spatial randomness of APs and UEs, and more importantly *3)* the interaction between the time domain and the spatial domain.
- Based on the above framework, we present a new heterogeneous MHCP model to analyse the inter-cell interference when LTE and Wi-Fi share the same bandwidth. Using this model, we derive the performance of a co-existing architecture where Wi-Fi coexists with an ideal CSMA duplex (ID-CSMA) systems, which achieves an upper bound performance for the LTE Release 14 LAA systems.
- Moreover, we derive the theoretical results on the performance of *Boost*, the predecessor of LWIP, which uses DL on Wi-Fi and UL on LTE.
- By analysing the network performance of traditional disjoint LTE and Wi-Fi architecture, the coexisting architecture and *Boost*, we can quantify the performance gain of these various strategies in terms of area system throughput (AST), which sheds valuable insights on the inter-working of LTE and Wi-Fi systems.

D. Paper Structure

The rest of the paper is organised as follows: In Section II, the system model and three different network architectures are described. In Section III, the existing results for LTE system performance analysis are presented, while the network performance of traditional Wi-Fi networks is studied in Section IV. Then the performance of coexisting Wi-Fi and ID-CSMA systems and the proposed *Boost* technology are studied in Section V and VI, respectively. In Section VII and VIII, the analysis results and conclusions are discussed, respectively.

II. Inter-working Strategies and System Model

In this section, we present the inter-working strategies and system model used in this paper.

A. The Analysed Inter-Working Strategies

Inline with the introduction, two *unlicensed* technologies are analysed in this paper, namely ID-CSMA and *Boost*.

1) ID-CSMA Systems in Unlicensed Spectrum: In contrast to the standardised LAA technology in LTE Release 13, which only supports LTE DL transmission in the unlicensed bands, we consider a system that supports both DL and UL transmissions and falls within the scope of LAA technology in LTE Release 14. Since the details of the UL transmission for LAA cells in LTE Release 14 are still under investigation/development, we model instead the performance of an idealised LAA-like system, referred to as ID-CSMA system, which gives an upper bound performance of the LAA technology in LTE Release 14, and can be used as a reference for system design.

The UL transmissions in this ID-CSMA system are assumed to be well-scheduled under the assistance of the licensed band,

as the DL transmissions in LAA Release 13. Fig. 1 shows an example of data transmission in the considered ID-CSMA system, where the cell uses the CCA to ensure the channel is idle before transmission and the random back-off scheme to avoid collisions among cells. When the ID-CSMA cell gains access to the channel, it transmits control signalling containing scheduling information for the DL or the UL (i.e., PDCCH or PUCCH), followed by the actual UE data (i.e., PDSCH or PUSCH) within the maximum channel occupancy time. The assumption is that no LBT is used at the UE, which as mentioned earlier should reflect the upper bound performance.

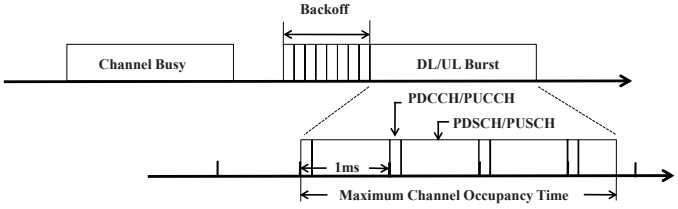

Fig. 1. An illustration of an ID-CSMA data transmission.

2) Boost: Boost is a brand-new technology that uses DL on Wi-Fi and UL on LTE [18]. As shown in Fig. 2, by redirecting UL traffic from the Wi-Fi network in the unlicensed band to the LTE network in the licensed band, Wi-Fi operates only in the DL and works on a centralised scheduled basis (DL Wi-Fi traffic is currently scheduled by the Wi-Fi AP). This allows an efficient use of Wi-Fi's large bandwidth, without the delay introduced by UL contention and in a completely collision-free manner inside a cell. In this way, *Boost* allows operators to combine stand-alone Wi-Fi and LTE networks into one unified wireless network for home, office and outdoor environments, and only requires software updates at the network and the UE [19].

B. Network Model

Let us consider a network comprised of licensed and unlicensed spectrum. The licensed bandwidth used by the LTE system is denoted by B^L, while the unlicensed bandwidth used by the Wi-Fi/ID-CSMA system is denoted by B^W. The frequency reuse factor of the LTE systems is 1, while the available bandwidth of the Wi-Fi/ID-CSMA system is divided into M non-overlapping channels according to the 802.11 specifications. In other words, each LTE cell can use the entire licensed bandwidth, while the bandwidth that each Wi-Fi or ID-CSMA cell can use is B^W/M.

The distributions of LTE BSs, ID-CSMA BSs and Wi-Fi APs are modelled as independent HPPPs with intensity λ_s^L, λ_s^A and λ_s^W, respectively.

The transmission powers of LTE BSs, ID-CSMA BSs and Wi-Fi APs are denoted by P_s^L, P_s^A and P_s^W, respectively. while the transmission powers of LTE UEs, ID-CSMA UEs and Wi-Fi UEs are denoted by P_u^L, P_u^A or P_u^W, respectively.

C. Network Architectures

In this paper, we consider three network architectures corresponding to the different LTE and Wi-Fi inter-working strategies as follows.

1) The Traditional Architecture: In this architecture, the LTE and the Wi-Fi systems work independently. The distributions of UEs that connect with LTE BSs and Wi-Fi APs are modelled as independent HPPPs with intensities λ_u^L and λ_u^W, respectively. It is important to note that an FDD LTE system is considered where the licensed bandwidth of LTE is split into two parts, i.e., the bandwidth for UL transmissions is ςB^L, while the bandwidth for DL transmissions is $(1-\varsigma)B^L$.

2) The Coexisting Architecture: In this architecture, LTE BSs work in the licensed spectrum, while ID-CSMA BSs and Wi-Fi APs coexist in the unlicensed spectrum. The UEs in the unlicensed band with density λ_u^W can be served by ID-CSMA BSs or Wi-Fi APs. Following the co-existence spirit in the 3GPP specifications, an LAA cell should not impact Wi-Fi services more than an additional Wi-Fi cell on the same carrier, and thus we assume that $P_s^A = P_s^W$ and $P_u^A = P_u^W$.

3) The Boost Architecture: With *Boost*, all the UL traffic is served by LTE, while all the DL traffic is served by Wi-Fi. As a result, the whole LTE bandwidth B^L is used for the LTE UL, the density of UEs served by either LTE or Wi-Fi is $\lambda_u = \lambda_u^L + \lambda_u^W$, and the intra-cell collision is completely avoided in Wi-Fi due to the centralised DL scheduling at the Wi-Fi APs.

D. Channel Model

We assume that each BS/AP/UE is equipped with an isotropic antenna, and that the multi-path fading between an BS/AP and a UE is modelled as independently identical distributed (i.i.d.) Rayleigh fading.

The power received from a transmitter located at x at location y, denoted by $P(x,y)$, is

$$P(x,y) = P_t \cdot h(x,y) \cdot l(x,y), \tag{1}$$

where *1)* P_t is the transmission power, *2)* $h(x,y)$ is the multi-path fading from x to y, which is assumed to be exponentially distributed with a mean of one due to our consideration of Rayleigh fading, and *3)* $l(x,y) = L_0\|x-y\|^{-\alpha}$ is the path loss between x and y, where L_0 is the reference path loss at the unit distance, α is the path loss exponent, and $\|\cdot\|$ is the Euclidean norm. In more detail, the reference path loss values for the licensed and unlicensed spectrum are denoted by L_0^L and L_0^W, respectively, and the path loss exponents for the licensed and unlicensed spectrum are denoted by α^L and α^W, respectively.

It is important to note that in the traditional and coexisting architectures, since Wi-Fi works in a TDD mode, we have that $h(x,y) = h(y,x)$ due to the channel reciprocity for the DL and the UL.

E. UE Association

As a common practice in the field [17, 20], the nearest association scheme is adopted in this work. In more detail, in the traditional and coexisting architecture, UEs in the licensed band associate with their nearest LTE BS, while UEs in the unlicensed band associate with the nearest Wi-Fi AP or ID-CSMA BS since they have the same transmission power.

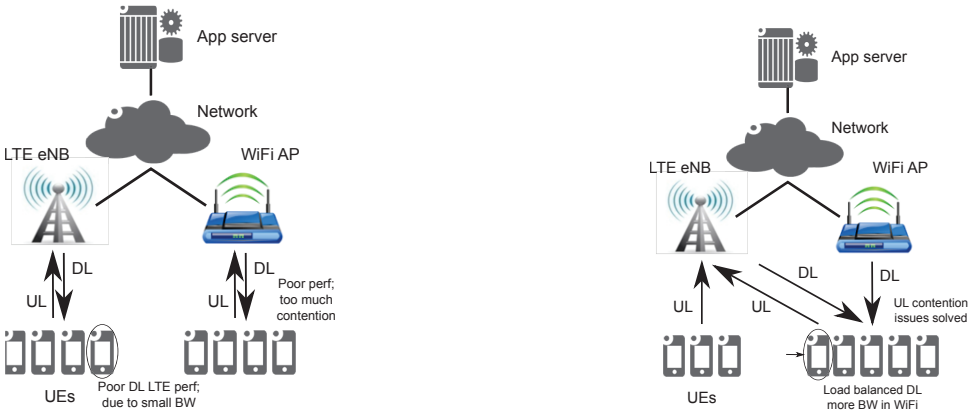

(a) Traditional architecture (b) *Boost* architecture

Fig. 2. *Boost* alleviates WiFi network congestion by diverting UL traffic to the LTE network. Moreover, it alleviates LTE DL congestion by moving DL traffic to the WiFi network with large bandwidth.

Therefore, the network plane is tessellated into two layer first-order Voronoi cells, i.e., the licensed and the unlicensed layer, where the first-order Voronoi cell $\mathcal{V}(x_i)$ associated with the BS/AP located at x_i, is defined as

$$\mathcal{V}(x_i) \triangleq \left\{ y \in \mathbb{R}^2 \mid \|y - x_i\| \leq \|y - x_j\|,\ \forall i \neq j \right\}. \quad (2)$$

III. Performance Analysis of LTE in the Traditional Architecture

In the traditional architecture, the network can be viewed as a stand-alone LTE system and a stand-alone Wi-Fi system operating on different frequency spectrum. Since the performance of LTE systems have been well studied in the literature, in the following, we directly show the existing results in terms of the average ergodic rate and then formulate the AST. Note that these existing results are derived based on the assumption that the density of UEs is sufficiently larger than that of BSs, which ensures that each BS has at least one UE to serve in its coverage area[2].

A. Average Ergodic Rate

In the following, we present the average ergodic rate for the DL and the UL.

1) Average Ergodic Rate in the DL: Denoted by γ_d^L the DL signal-to-interference-plus-noise ratio (SINR) in LTE, according to Theorem 3 in [9], the average ergodic rate of a typical UE in the DL, denoted by ρ_d^L, can be expressed by

$$\rho_d^L \triangleq \mathbb{E}\left[\ln(1+\gamma_d^L)\right] = \int_0^\infty 2\pi\lambda_s^L r \exp\left(-\pi\lambda_s^L r^2\right) \int_{t>0} \exp\left(-\frac{\sigma^2 r^{\alpha^L}}{P_s^L L_0^L}(e^t-1)\right) \cdot \mathcal{L}_{I_d}\left(\frac{r^{\alpha^L}}{P_s^L L_0^L}(e^t-1)\right) \mathrm{d}t\mathrm{d}r, \quad (3)$$

where

$$\mathcal{L}_{I_d}\left(\frac{r^{\alpha^L}}{P_s^L L_0^L}(e^t-1)\right) = \exp\left(-\pi\lambda_s^L r^2 (e^t-1)^{2/\alpha^L} \int_{(e^t-1)^{-2/\alpha^L}}^\infty \frac{1}{1+x^{\alpha^L/2}}\mathrm{d}x\right). \quad (4)$$

[2]In order to satisfy this constraint, we assume $\lambda_u^L > 4\lambda_s^L$ according to the distribution of the area of Voronoi cells in Eq. (9).

2) Average Ergodic Rate in the UL: Denoted by γ_u^L the UL SINR in LTE, according to [11], the average ergodic rate of a typical UE in the UL, denoted by ρ_u^L, can be written as

$$\rho_u^L \triangleq \mathbb{E}\left[\ln(1+\gamma_u^L)\right] = \int_0^\infty 2\pi\lambda_s^L r \exp\left(-\pi\lambda_s^L r^2\right) \int_{t>0} \exp\left(-\frac{\sigma^2(e^t-1)}{P_u^L(\frac{1}{L_0^L}r^{\alpha^L})^{(\epsilon-1)}}\right) \mathcal{L}_{I_u}\left(\frac{e^t-1}{P_u^L(\frac{1}{L_0^L}r^{\alpha^L})^{(\epsilon-1)}}\right) \mathrm{d}t\mathrm{d}r, \quad (5)$$

where $\epsilon \in [0,1]$ is the UL power control factor and

$$\mathcal{L}_{I_u}(s) = \exp\left(-2\pi\lambda_s^L \int_r^\infty \int_0^x 2\pi\lambda_s^L u \exp(-\lambda_s^L \pi u^2) \left(1 - \frac{1}{1+sP_u^L(\frac{1}{L_0^L}u^{\alpha^L})^\epsilon L_0^L x^{-\alpha^L}}\right) \mathrm{d}u x \mathrm{d}x\right). \quad (6)$$

B. Area System Throughput

Based on the average ergodic rates in the DL and the UL in (3) and (5), and considering the bandwidth allocated to the DL and UL, the system throughput per unit area, i.e., the area system throughput (AST), of the LTE system in the licensed band can be formulated as

$$AST^L = \lambda_s^L B^L \left(\varsigma\eta_u^L\rho_u^L + (1-\varsigma)\eta_d^L\rho_d^L\right), \quad (7)$$

where η_u^L and η_d^L are the effective resource utilization factors (less than one due to control signalling overhead) of the physical and MAC layers in the respective LTE UL and DL.

IV. Performance Analysis of Wi-Fi in the Traditional Architecture

The network performance of Wi-Fi, in terms of the average ergodic rate and the AST, jointly considering the DL and the UL as well as the time and the spatial domains, have not been investigated yet in the literature. For the first time, we tackle this problem and present our main results in the following.

A. Intra-Cell Analysis for Wi-Fi

We consider a typical UE located at the origin o, whose serving AP is located at x_0 with polar coordinates $(r, 0)$, where $r = \|x_0\|$. According to the Voronoi cell definition in (2), the cell managed by the AP located at x_0 is denoted by $\mathcal{V}(x_0)$. Due to the nearest association scheme, the probability density function (PDF) of r is given by

$$f(r) = 2\pi\lambda_s^W r \exp(-\lambda_s^W \pi r^2). \tag{8}$$

1) The Number of UEs Associated with an AP: We denote the area size of an AP's first-order Voronoi cell by s. According to [21], the PDF of s can be approximated as

$$f(s) = \frac{(\lambda_s^W K)^K}{\Gamma(K)} s^{(K-1)} \exp\left(-K\lambda_s^W s\right), \tag{9}$$

where $\Gamma(K) = \int_0^\infty x^{K-1}\exp(-x)\mathrm{d}x$ is the Gamma function, and $K \approx 3.575$.

Since the distribution of UEs follows an HPPP with an intensity of λ_u^W, given a Voronoi cell with area size s, the number of UEs located in this Voronoi cell should follow a Poisson random variable with mean $\lambda_u^W s$. Denoting by n the number of UEs located in a Voronoi cell, we have that

$$\begin{aligned}\Pr(n = N) &= \int_0^\infty \frac{(\lambda_u^W s)^N}{N!}\exp(-\lambda_u^W s) f(s)\mathrm{d}s \\ &= \frac{\Gamma(N+K)}{N!\cdot\Gamma(K)}\left(\frac{\lambda_u^W}{\lambda_u^W + K\lambda_s^W}\right)^N \left(1 - \frac{\lambda_u^W}{\lambda_u^W + K\lambda_s^W}\right)^K.\end{aligned} \tag{10}$$

From (10), we can see that the number of UEs located in a Voronoi cell, i.e., the number of UEs associated with an AP, follows a Negative Binomial distribution, which can be written as

$$n \sim \mathrm{NB}\left(K, \frac{\lambda_u^W}{\lambda_u^W + K\lambda_s^W}\right). \tag{11}$$

2) Probability of Activation a Wi-Fi AP: We only consider APs that have at least one UE to serve, i.e., active APs. Those APs serving no UE are ignored in our analysis since they do not inject effective transmissions into the network. Denoting by $\mathcal{A}$ that an AP is active, the probability of activation $\Pr(\mathcal{A})$ can be calculated by

$$\begin{aligned}A \triangleq \Pr(\mathcal{A}) &= \Pr[n \neq 0] = 1 - \Pr[n = 0] \\ &= 1 - \left(1 - \frac{\lambda_u^W}{\lambda_u^W + K\lambda_s^W}\right)^K.\end{aligned} \tag{12}$$

3) Time Efficiency Inside a Wi-Fi Cell: Under the CSMA/CA protocol, there are three kinds of status for a Wi-Fi cell: idle, transmission and collision [12, 13]. Without considering the capture effect, we define the time efficiency of a Wi-Fi cell as the time fraction that it is in the transmission status.

Assuming there are n UEs served by an AP, these $n+1$ nodes, i.e., n UEs plus the AP, will contend to access the channel with equal priority. Let us denote by ξ the probability that one node is in the status of transmission at a given time instance. Statistically speaking, ξ equals to the time fraction of transmission of such node. Obviously, ξ depends on the number of nodes in this Wi-Fi cell n, and thus should be denoted as $\xi(n)$. Regarding $\xi(n)$, we have two remarks as follows,

- The time fraction of transmission for each node decreases with the growth of n.
- The time efficiency of the Wi-Fi system, i.e., $(n+1)\xi(n)$, decreases with the growth of n [12, 13].

Moreover, let us denote by $\vartheta(n)$ the probability that a Wi-Fi cell is in the status of collision at a given time instance. Since a larger number of nodes implies a higher probability of collision, it monotonically increases with the number of nodes $n+1$. One analytical example about the impact of the number of nodes $n+1$ on the system utility can be found in Fig. 6 of [12]. Moreover, we present the analytical results of $\xi(n)$, $(n+1)\xi(n)$ and $\vartheta(n)$ based on the well-known Bianchi's model [12] in Appendix A.

B. Inter-Cell Analysis for Wi-Fi

Due to the CSMA protocol, the channel contention also occurs among the nodes working in different co-channel Wi-Fi cells. These inter-cell contentions imply that:

- Not all of the co-channel cells can transmit simultaneously.
- The inter-cell interference only comes from the co-channel cells that successfully grab the opportunities to transmit.

1) Model for Interfering Wi-Fi Cells: In this subsection, we analyse the channel contention among co-channel Wi-Fi cells. According to the carrier sensing protocol adopted by Wi-Fi, $\mathcal{V}(x_j)$ is inside the contention domain of $\mathcal{V}(x_i)$, if the received power $P\left(\mathcal{V}(x_j), \mathcal{V}(x_i)\right)$ is larger than a threshold Γ, where Γ denotes the CCA threshold. In such case, $\mathcal{V}(x_j)$ and $\mathcal{V}(x_i)$ cannot transmit simultaneously.

For tractability, we abstract a Wi-Fi cell as a spatial point and use the centre of a Wi-Fi cell, i.e., the location of its AP, to represent its location. In addition, we use the expected transmission power inside this Wi-Fi cell to approximately represent the cell's transmission power. Thus, given n_j UE in $\mathcal{V}(x_j)$, we have

$$P\left(\mathcal{V}(x_j), \mathcal{V}(x_i)\right) \triangleq \frac{n_j P_u^W + P_s^W}{n_j + 1} \cdot h(x_j, x_i) \cdot \|x_j - x_i\|^{-\alpha^W}. \tag{13}$$

In (13), the inter-cell distance is sufficiently accurate because the distance between two co-channel Wi-Fi cell is much larger than the average range of a Wi-Fi cell coverage, especially when M is large. Besides, the usage of the expected transmission power is reasonable since the transmission powers of a AP and an UE are comparable in practical Wi-Fi networks.

Among the Wi-Fi cells in contention, the cell with the node which has the minimum back-off time will seize this channel. By introducing a random mark to represent the minimum back-off time inside a cell, a modified MHCP Type II can be used to model the positions of cells that grab the opportunities to transmit in a time instance [16].

The modified MHCP is generated following similar steps as in [22]: Firstly, an independent random mark $m(\cdot)$, uniformed

distributed in $[0,1]$, is tagged onto each point, i.e., each co-channel cell, in an HPPP. Secondly, all points that have a neighbouring point with a smaller mark and within its contention domain are removed.

Denoting by ϕ_{x_0} the position of the Wi-Fi cells that attempt to access the same channel as the typical cell $\mathcal{V}(x_0)$ including x_0, and $\phi_{x_0}^M$ the positions of the Wi-Fi cells that successfully grab the opportunities to transmit in a time instance, i.e., retained in a modified MHCP, we have

$$\phi_{x_0}^M \triangleq \{x_i \in \phi_{x_0} : \\ m(x_i) < m(x_j) \text{ and } P\left(\mathcal{V}(x_j), \mathcal{V}(x_i)\right) > \Gamma, \forall x_j \in \phi_{x_0}\}. \tag{14}$$

Hence, when the typical cell is transmitting, the positions of its interfering Wi-Fi cells, denoted by $\phi_{x_0}^I$, can be formulated as $\phi_{x_0}^I = \left\{x_i : x_i \in \phi_{x_0}^M \mid x_0 \in \phi_{x_0}^M, x_i \neq x_0\right\}$.

2) Inter-Cell Interference of Wi-Fi: Let us consider an interfering cell $\mathcal{V}(x_i)$ of the typical cell $\mathcal{V}(x_0)$. Denoting by n_i the number of UEs in $\mathcal{V}(x_i)$, and $x_{i,j}$ the location of the j-th UE in it, where $1 \leq j \leq n_i$, the interference from the Wi-Fi cell $\mathcal{V}(x_i)$ to $\mathcal{V}(x_0)$ may come from three sources: *1)* UL transmissions from the UEs, or *2)* DL transmission from the AP, or *3)* the nodes transmitting together during a collision.

The transmission powers in the UL and DL transmissions are P_u^W and P_s^W, respectively, while the transmission power during a collision depends on the number of nodes involved. Since most collisions are 2-node collisions, for simplicity, a virtual node located at the centre of a Wi-Fi cell with doubled expected transmission power is used to represent the interfering source during collided transmissions.

Taking into account the possible interference sources, the probability that each interference source occurs, the transmission power and the location of each source, the aggregate interference power received at the typical UE in the Wi-Fi DL, denoted by I_d, can be formulated as

$$\begin{aligned} I_d \approx & \sum_{x_i \in \phi_{x_0}^I} \Bigg(\xi(n_i) P_s^W h_i L_0^W \|x_i\|^{-\alpha^W} \\ & + \sum_{x_{i,j} \in \mathcal{V}(x_i)} \xi(n_i) P_u^W h_{i,j} L_0^W \|x_{i,j}\|^{-\alpha^W} \\ & + \vartheta(n_i) P_{x_i}^{col} h_{i,i} L_0^W \|x_i\|^{-\alpha^W} \Bigg) \\ \approx & \sum_{x_i \in \phi_{x_0}^I : \|x_i\| > r} L_0^W \|x_i\|^{-\alpha} \Bigg(\xi(n_i) P_s^W h_i \\ & + \sum_{j=1}^{n_i} \xi(n_i) P_u^W h_{i,j} + \vartheta(n_i) 2 \frac{n_i P_u^W + P_s^W}{n_i + 1} h_{i,i} \Bigg), \end{aligned} \tag{15}$$

where h_i, $h_{i,j}$, and $h_{i,i}$ are the channel fading from the AP located at x_i, the channel fading from the UE located at $x_{i,j}$, and the channel fading from the virtual collision interfering node to the target UE, respectively. Moreover, $P_{x_i}^{col} = 2\frac{n_i P_u^W + P_s^W}{n_i + 1}$ is the transmission power during collisions, and $\|x_i\| > r$ ensures that the nearest AP serves the typical UE. Note that the second approximation comes from the fact that $\|x_{i,j}\| \approx \|x_i\|$. This approximation is generally accurate because the distance between two interfering cells is usually much larger than the range of a Wi-Fi cell coverage.

Similar as in the previous formulation, the aggregate interference power received at the AP located at x_0 in the Wi-Fi UL, denoted by I_u , can be formulated as

$$\begin{aligned} I_u \approx & \sum_{x_i \in \phi_{x_0}^I} \Bigg(\xi(n_i) P_s^W h_i^{'} L_0^W \|x_i - x_0\|^{-\alpha^W} \\ & + \sum_{x_{i,j} \in \mathcal{V}(x_i)} \xi(n_i) P_u^W h_{i,j}^{'} L_0^W \|x_{i,j} - x_0\|^{-\alpha^W} \\ & + \vartheta(n_i) P_{x_i}^{col} h_{i,i}^{'} L_0^W \|x_i - x_0\|^{-\alpha^W} \Bigg) \\ \approx & \sum_{x_i \in \phi_{x_0}^I : \|x_i\| > r} L_0^W \|x_i - x_0\|^{-\alpha^W} \Bigg(\xi(n_i) P_s^W h_i^{'} \\ & + \sum_{j=1}^{n_i} \xi(n_i) P_u^W h_{i,j}^{'} + \vartheta(n_i) 2 \frac{n_i P_u^W + P_s^W}{n_i + 1} h_{i,i}^{'} \Bigg), \end{aligned} \tag{16}$$

where $h_i^{'}$, $h_{i,j}^{'}$, and $h_{i,i}^{'}$ are the channel fading from the AP x_i, the channel fading from the UE $x_{i,j}$, and the channel fading from the virtual transmitter during collisions. As with the approximation in (15), the second approximation in (16) is based on the fact that $\|x_{i,j} - x_0\| \approx \|x_i - x_0\|$.

C. Laplace Transform of The Aggregate Interference

In order to analyse the aggregate interference, we firstly analyse the probability that a co-channel cell $\mathcal{V}(x_i)$ at a distance z to the typical cell becomes one of the interfering cells.

Lemma 1. *Given that the typical cell is transmitting, the probability that a co-channel cell at distance z to the typical cell is also granted transmission, i.e., retained in $\phi_{x_0}^I$, is given by*

$$\begin{aligned} \kappa(z) = & \left(\frac{\exp(-C)}{-C} + \frac{1 - \exp(-B(z))}{CB(z)} + \frac{1}{B(z)} \right. \\ & \left. + \frac{\exp(-B(z)) - 1}{B^2(z)} \right) \cdot \left(1 - \exp\left(\frac{-\Gamma}{P_{ave}^W L_0^W z^{-\alpha^W}} \right) \right), \end{aligned} \tag{17}$$

where $C = \frac{A}{M} \lambda_s^W c$, $B(z) = \frac{A}{M} \lambda_s^W (b(z) - c)$, and

$$b(z) = 2c - \int_0^\infty \int_0^{2\pi} \exp\Bigg(- \frac{\Gamma}{P_{ave}^W L_0^W} \\ \left(\tau^{\alpha^W} + \left(\tau^2 + z^2 - 2\tau z \cos\omega \right)^{\alpha^W/2} \right) \Bigg) \tau d\omega d\tau, \tag{18}$$

and

$$c = 2\pi \int_0^\infty \exp\left(- \frac{\Gamma}{P_{ave}^W L_0^W y^{-\alpha^W}} \right) y dy, \tag{19}$$

and

$$P_{ave}^W = \frac{\sum_{N=1}^\infty \Pr(n = N) \frac{N P_u^W + P_s^W}{N+1}}{\Pr(n \neq 0)}. \tag{20}$$

Proof: See Appendix B.

Based on the retained probability in (17), and the assumption that each co-channel cell is retained independently, we have the following theorem on the Laplace transform of the aggregate interference.

Theorem 1. *The Laplace transform for the aggregate interference I_d and I_u is*

$$\begin{aligned}\mathcal{L}^r_{I_d}(s) &= \mathcal{L}^r_I(s)\big|_{g=l},\\ \mathcal{L}^r_{I_u}(s) &= \mathcal{L}^r_I(s)\big|_{g=\sqrt{r^2+l^2-2rl\cos\theta}},\end{aligned} \tag{21}$$

where $\mathcal{L}^r_I(s)$ given by (22), shown on the top of next page.

Proof: See Appendix C.

D. SINR Distribution

In this section, the DL and UL SINR distribution for the nodes within the typical Wi-Fi cell are obtained.

1) Distribution of the DL SINR: Denoted by h_0 the channel fading between the AP and the typical UE, we can formulate the DL received SINR at the typical UE as

$$\gamma^W_d = \frac{P^W_s h_0 L^W_0 \|x_0\|^{-\alpha^W}}{I_d+\sigma^2} = \frac{P^W_s h_0 L^W_0 r^{-\alpha^W}}{I_d+\sigma^2}, \tag{23}$$

where σ^2 denotes the noise power. Therefore, the CCDF of the DL SINR is given by

$$\begin{aligned}\Pr\left[\gamma^W_d \geq \delta\right] &= \int_0^\infty \Pr\left[\frac{P^W_s h_0 L^W_0 r^{-\alpha^W}}{I_d+\sigma^2} \geqslant \delta\right] f(r)\mathrm{d}r\\ &= \int_0^\infty \mathcal{L}^r_{I_d}\left(\frac{r^\alpha \delta}{P^W_s L_0}\right)\exp\left(-\frac{r^\alpha\delta\sigma^2}{P^W_s L_0}\right)\\ &\quad\cdot 2\pi\lambda^W_s r\exp\Big(-\pi\lambda^W_s r^2\Big)\mathrm{d}r.\end{aligned} \tag{24}$$

2) Distribution of the UL SINR: As the channel fading for the UL and the DL is the same due to the TDD nature of Wi-Fi, we can formulate the UL receive SINR at the AP x_0 as

$$\gamma^W_u = \frac{P^W_u h_0 L^W_0 \|x_0\|^{-\alpha^W}}{I_u+\sigma^2} = \frac{P^W_u h_0 L^W_0 r^{-\alpha^W}}{I_u+\sigma^2}. \tag{25}$$

Therefore, the CCDF of the UL SINR is given by

$$\begin{aligned}\Pr\left[\gamma^W_u \geq \delta\right] &= \int_0^\infty \mathcal{L}^r_{I_u}\left(\frac{r^\alpha \delta}{P^W_u L_0}\right)\exp\left(-\frac{r^\alpha\delta\sigma^2}{P^W_u L_0}\right)\\ &\quad\cdot 2\pi\lambda^W_s r\exp\Big(-\pi\lambda^W_s r^2\Big)\mathrm{d}r.\end{aligned} \tag{26}$$

E. Area System Throughput

In this section, the DL and UL average ergodic rates for the nodes within the typical Wi-Fi cell are obtained as well as the AST.

1) Average Ergodic Rate in DL: Since the DL transmission time fraction equals $\xi(n_0)$, the DL average ergodic rate in the typical cell $\mathcal{V}(x_0)$ with n_0 UEs can be computed as $\rho^W_d \triangleq \mathbb{E}_{n_0\geq 1,\gamma^W_d}\left[\xi(n_0)\ln(1+\gamma^W_d)\right]$, where $n_0 \geq 1$ implies that the cell is an active cell. In more detail, we have

$$\begin{aligned}\rho^W_d &= \mathbb{E}_{n_0\geq 1}\left[\xi(n_0)\right]\cdot\mathbb{E}_{\gamma^W_d}\left[\ln(1+\gamma^W_d)\right]\\ &= \mathbb{E}_{n_0\geq 1}\left[\xi(n_0)\right]\int_0^\infty 2\pi\lambda^W_s r\exp\Big(-\pi\lambda^W_s r^2\Big)\int_0^\infty\\ &\exp\left(-\frac{r^{\alpha^W}\sigma^2}{P^W_s L^W_0}(e^t-1)\right)\mathcal{L}^r_{I_d}\left(\frac{r^{\alpha^W}}{P^W_s L^W_0}(e^t-1)\right)\mathrm{d}t\mathrm{d}r.\end{aligned} \tag{27}$$

2) Average Ergodic Rate in UL: Since statistically $\xi(n_0)$ equals to the time fraction of transmission of each UE, the UL transmission time fraction in the typical cell $\mathcal{V}(x_0)$ equals to $n_0\xi(n_0)$. Thus, the UL average ergodic rate in the typical cell $\mathcal{V}(x_0)$ can be given by

$$\begin{aligned}\rho^W_u &\triangleq \mathbb{E}_{n_0\geq 1,\gamma^W_u}\left[n_0\xi(n_0)\ln(1+\gamma^W_u)\right]\\ &= \mathbb{E}_{n_0\geq 1}\left[n_0\xi(n_0)\right]\int_0^\infty 2\pi\lambda^W_s r\exp(-\pi\lambda^W_s r^2)\int_0^\infty\\ &\exp\left(-\frac{r^{\alpha^W}\sigma^2}{P^W_u L^W_0}(e^t-1)\right)\mathcal{L}^r_{I_u}\left(\frac{r^{\alpha^W}}{P^W_u L^W_0}(e^t-1)\right)\mathrm{d}t\mathrm{d}r.\end{aligned} \tag{28}$$

3) Area System Throughput: Let us denote by η^W the efficiency (overhead loss) of Wi-Fi, which equals to the time fraction spent on transmitting user data. Since the bandwidth that the typical cell occupies is B^W/M, the throughput in the transmitting typical cell can be formulated as $\eta^W\cdot\frac{B^W}{M}\left(\rho^W_d+\rho^W_u\right)$.

Denoted by $\Pr(\mathcal{T}) \triangleq \Pr_{x_0}\left\{x_0\in\phi^M_{x_0}\right\}$ the probability that the typical Wi-Fi cell is granted transmission in the channel contentions with other co-channel cells, and considering the intensity of active cells, $A\lambda^W_s$, we can obtain the AST for WiFi in the unlicensed band as

$$AST^W = A\lambda^W_s\cdot\Pr(\mathcal{T})\cdot\eta^W\cdot\frac{B^W}{M}\left(\rho^W_d+\rho^W_u\right), \tag{29}$$

where $\Pr(\mathcal{T}) = \frac{1-\exp(-C)}{C}$ according to [16].

V. Network Performance Analysis of the Coexisting Architecture

In this architecture, some extra signalling in the licensed band is needed to assist the ID-CSMA system and pointing out the resources that are in used in the unlicensed band. The carrier aggregation signalling and scheduling framework can be used for this purpose. Since according to [23], the overhead of such signalling and scheduling is very limited and has a minor impact on the overall system performance, we assume in our work that the performance of LTE in the licensed band remains unaffected. Thus, we focus on the performance in the unlicensed band, where ID-CSMA BSs and Wi-Fi APs constitute a heterogeneous network. Let us remind that the distributions of the ID-CSMA BSs and the Wi-Fi APs are denoted by two independent HPPPs Φ^A and Φ^W, respectively, with intensities λ^A_s and λ^W_s.

$$\mathcal{L}_I^r(s) = \mathbb{E}_I\left[\exp\left(-sI\right)\right] \approx \sum_{N=1}^{\infty} \Pr\left(n=N\right) \exp\left(-\frac{A\lambda_s^W}{M}\int_0^{2\pi}\int_r^{\infty} \kappa\left(\sqrt{r^2+l^2-2rl\cos\theta}\right)\right.$$
$$\left.\left(1-\frac{1}{\left(1+s\xi(N)P_s^W L_0^W g^{-\alpha^W}\right)\left(1+s\xi(N)P_u^W L_0^W g^{-\alpha^W}\right)^N\left(1+s2\vartheta(N)\frac{NP_u^W+P_s^W}{N+1}L_0^W g^{-\alpha^W}\right)}\right) l\mathrm{d}l\mathrm{d}\theta\right). \tag{22}$$

A. Intra-Cell Analysis

Under the assumption $P_s^W = P_s^A$ and the nearest association scheme, the PDF of the distance between a UE and its serving ID-CSMA BS or Wi-Fi AP, $\hat{r}$, is given by [24]

$$f(\hat{r}) = 2\pi(\lambda_s^A+\lambda_s^W)\hat{r}\exp\left(-\pi\left(\lambda_s^W+\lambda_s^A\right)\hat{r}^2\right). \tag{30}$$

Since the intensity of serving nodes (BSs or APs) is $\lambda_s^A+\lambda_s^W$ in the coexisting architecture, the number of UEs in an ID-CSMA or a Wi-Fi cell, n, which follows the Negative Binomial distribution, can be written as

$$\hat{n} \sim \mathrm{NB}\left(K, \frac{\lambda_u^W}{\lambda_u^W + K\left(\lambda_s^A+\lambda_s^W\right)}\right). \tag{31}$$

Hence, the activation probability for a ID-CSMA BS or a Wi-Fi AP is given by

$$\hat{A} = 1-\left(1-\frac{\lambda_u^W}{\lambda_u^W + K\left(\lambda_s^A+\lambda_s^W\right)}\right)^K. \tag{32}$$

Inside a Wi-Fi cell, the AP and the UEs contend for the channel under CSMA/CA protocols, which has been analysed in Subsection IV.A. In contrast, we assume that the DL and UL transmissions are well scheduled inside an ID-CSMA cell under the assistance of the LTE BSs, and thus there is no need for CSMA/CA protocols inside an ID-CSMA cell (see Section II and Fig. 1). For simplicity, we assume that one half of the transmission time inside an ID-CSMA cell is used for the DL transmissions while the other half is used for the UL transmissions.

B. Inter-Cell Analysis for the Coexistence of ID-CSMA and Wi-Fi

1) Heterogeneous MHCP: Due to CSMA/CA, the channel contention among the ID-CSMA and Wi-Fi cells in the coexisting architecture is similar with that among Wi-Fi cells in the traditional architecture, and hence, the MHCP model can also be used to analyse the inter-cell interference in the coexisting architecture. However, considering the two different kinds of cells, i.e. ID-CSMA and Wi-Fi cells, involved in the contention, a heterogeneous MHCP is adopted.

As mentioned before, in the analysis of the inter-cell channel contention, each cell is abstracted to a point located at its centre with its expected transmission power. Since in an ID-CSMA cell one half of the transmission time is scheduled for DL and the other half is scheduled for UL, the expected power of an ID-CSMA cell is given by $P_{ave}^A = (P_s^W + P_u^W)/2$, which is different from the expected power of a Wi-Fi cell with n UEs formulated as: $P_{ave}^W = \frac{P_s^W + nP_u^W}{n+1}$ (see Section IV.B1). Moreover, the intensities of ID-CSMA and Wi-Fi cells involved into channel contentions are $\frac{\hat{A}}{M}\lambda_s^A$ and $\frac{\hat{A}}{M}\lambda_s^W$, respectively.

Considering these difference of the cells involved in the channel contention, in the coexisting architecture, the cells granted to transmission in a time instance constitute a heterogeneous MHCP. Compared with the modified MHCP model used in the traditional Wi-Fi network, the heterogeneous MHCP model considers different expected transmission powers and intensities for different types of cells that are involved in the channel contentions.

2) Aggregate Inter-cell Interference: Given the typical cell $\mathcal{V}(x_0)$ grabs the opportunity to transmission, i.e., retained in the heterogeneous MHCP $\hat{\phi}_{x_0}^M$, the positions of its interfering cells can be modelled as $\hat{\phi}_{x_0}^I = \left\{x_i : x_i \in \hat{\phi}_{x_0}^M \mid x_0 \in \hat{\phi}_{x_0}^M, x_i \neq x_0\right\}$. The inter-cell interference comes from two parts: the interfering ID-CSMA cells, i.e. $\hat{\phi}_{x_0}^I \cap \Phi^A$, and the interfering Wi-Fi cells, $\hat{\phi}_{x_0}^I \cap \Phi^W$, which are denoted by $\hat{I}_1$ and $\hat{I}_2$, respectively.

For the interference from Wi-Fi cells, $\hat{I}_2$, as we mentioned in the previous section, it comes from three possible sources (see Subsection IV.B2). In contrast, for $\hat{I}_1$, the interference caused by an ID-CSMA cell comes from two possible sources: its ULs and DLs due to its well-scheduling feature, no collisions. Under the assumption of TDD mode, the ID-CSMA BS transmits with probability $1/2$, and each UE transmits with probability $\frac{1}{2\hat{n}}$, where $\hat{n}$ denotes the UE number in the cell.

Let us denoted by χ the receiver's location in the typical cell $\mathcal{V}(x_0)$, then the aggregate inter-cell interference received at χ can be formulated as

$$\begin{aligned}\hat{I} = \hat{I}_1 + \hat{I}_2 \approx & \sum_{y_i \in \hat{\phi}_{x_0}^I \cap \Phi^A} \left(\frac{1}{2}P_s^W h_i' L_0^W \left\|y_i-\chi\right\|^{-\alpha^W}\right. \\ & \left. + \sum_{y_{i,j}\in\mathcal{V}(y_i)} \frac{1}{2\cdot n_i'} P_u^W h_{i,j}' L_0^W \left\|y_{i,j}-\chi\right\|^{-\alpha^W}\right) \\ & + \sum_{x_i \in \hat{\phi}_{x_0}^I \cap \Phi^W} \left(\sum_{x_{i,j}\in\mathcal{V}(x_i)} \xi(n_i) P_u^W h_{i,j} L_0^W \left\|x_{i,j}-\chi\right\|^{-\alpha^W}\right. \\ & \left. + \left(\xi(n_i)P_s^W h_i + \vartheta(n_i)\hat{P}_{x_i}^{col} h_{i,i}\right) L_0^W \left\|x_i-\chi\right\|^{-\alpha^W}\right).\end{aligned} \tag{33}$$

With $\chi = 0$, we can obtain the aggregate inter-cell interference suffered by the typical UE, i.e., the interference for the DL transmission in the typical cell. With $\chi = x_0$, we can obtain the interference for the UL transmission in the typical cell. Due to the nearest association, we have two constraints: $\|y_i\| > r$ and $\|x_i\| > r$.

C. Laplace Transform of the Aggregate Interference in a Heterogeneous MHCP

1) Retained Probability of a Co-Channel Cell: Compared with the modified MHCP studied in previous section, in the heterogeneous MHCP, the probability that a co-channel cell is retained in $\hat{\phi}^I_{x_0}$ has to consider the type of the typical cell as well as the type of this co-channel cell. That is, the typical cell $\mathcal{V}(x_0)$ is an ID-CSMA or a Wi-Fi cell, and the co-channel cell $\mathcal{V}(x_i)$ is an ID-CSMA or a Wi-Fi cell. In more detail, we have the following lemma to calculate the retained probability of a co-channel cell.

Lemma 2. *Consider a heterogeneous MHCP, which is retained from the point process consisting of two independent HPPPs, Φ^W and Φ^A, with intensities $\frac{\hat{A}}{M}\lambda_s^W$ and $\frac{\hat{A}}{M}\lambda_s^A$, and with transmission powers P_{ave}^W and P_{ave}^A, respectively. Given a retained point x_0, the probability to retain the point x_i with a distance z from x_0, can be obtained as*

$$\hat{\kappa}(z)=\begin{cases}\kappa_{AW}(z)=\upsilon_1(z)\cdot\varsigma_A(z)+\upsilon_2(z)\cdot\varsigma_W(z),\\ \qquad\qquad \textit{if } x_0\in\Phi^A, x_i\in\Phi^W\\ \kappa_{AA}(z)=\upsilon_1(z)\cdot\varsigma_A(z)+\upsilon_2(z)\cdot\varsigma_A(z),\\ \qquad\qquad \textit{if } x_0\in\Phi^A, x_i\in\Phi^A\\ \kappa_{WA}(z)=\upsilon_1(z)\cdot\varsigma_W(z)+\upsilon_2(z)\cdot\varsigma_A(z),\\ \qquad\qquad \textit{if } x_0\in\Phi^W, x_i\in\Phi^A\\ \kappa_{WW}(z)=\upsilon_1(z)\cdot\varsigma_W(z)+\upsilon_2(z)\cdot\varsigma_W(z),\\ \qquad\qquad \textit{if } x_0\in\Phi^W, x_i\in\Phi^W\end{cases} \tag{34}$$

where

$$\upsilon_1(z)=-\frac{\exp\left(-C^{'}\right)}{C^{'}}-\frac{\exp\left(-B^{'}(z)\right)-1}{C^{'}B^{'}(z)},$$

$$\upsilon_2(z)=\frac{\exp\left(-B^{'}(z)\right)-1}{\left(B^{'}(z)\right)^2}+\frac{1}{B^{'}(z)},$$

and

$$\varsigma_A(z)=1-\exp\left(-\frac{\Gamma}{P_{ave}^A L_0^W z^{-\alpha^W}}\right),$$

$$\varsigma_W(z)=1-\exp\left(-\frac{\Gamma}{P_{ave}^W L_0^W z^{-\alpha^W}}\right).$$

Moreover, we can have that $C^{'}=\frac{\hat{A}}{M}\left(\lambda_s^W c_1+\lambda_s^A c_2\right)$ and $B^{'}(z)=\frac{\hat{A}}{M}\left(\lambda_s^W\left(b_1(z)-c_1\right)+\lambda_s^A\left(b_2(z)-c_2\right)\right)$, where $c_1=c$ in Eq.(19), $b_1(z)=b(z)$ in Eq.(18), and

$$c_2=2\pi\int_0^\infty\exp\left(-\frac{\Gamma}{P_{ave}^A L_0^W l^{-\alpha^W}}\right)l dl,$$

and

$$b_2(z)=2c_2-\int_0^\infty\int_0^{2\pi}\exp\Bigg(-\frac{\Gamma}{P_{ave}^A L_0^W}\left(\tau^{\alpha^W}+\left(\tau^2+z^2-2\tau z\cos\omega\right)^{\alpha^W/2}\right)\Bigg)\tau d\omega d\tau.$$

Proof: See Appendix B.

2) Laplace Transform of the Aggregate Interference: The aggregate interference from the co-channel Wi-Fi cells, $\hat{I}_2$ in (33), has a similar formulation compared with the aggregate interference in the traditional architecture. Thus, we can formulate the Laplace transform of $\hat{I}_2$ as the expressions in **Theorem 1** by substituting the retained probability in the heterogeneous MHCP, i.e., $\hat{\kappa}(\cdot)$ in (34).

Moreover, the Laplace transform of the aggregate interference from the co-channel ID-CSMA cells can be formulated as

$$\mathcal{L}^{\hat{r}}_{\hat{I}_1}(s)=\sum_{N=1}^{\infty}\Pr(n=N)\exp\Bigg(-\frac{\hat{A}\lambda_s^A}{M}\int_0^{2\pi}\int_{\hat{r}}^{\infty}\left(1-\frac{1}{\left(1+\frac{s}{2}P_s^W L_0^W g^{-\alpha^A}\right)\left(1+\frac{s}{2N}P_u^W L_0^W g^{-\alpha^A}\right)^N}\right)\hat{\kappa}\left(\sqrt{\hat{r}^2+l^2-2\hat{r}l\cos\theta}\right)l dl d\theta\Bigg). \tag{35}$$

Note that, similar to **Theorem 1**, $g=l$ when considering the inter-cell interference for the DL transmission in the typical cell, while $g=\sqrt{\hat{r}^2+l^2-2\hat{r}l\cos\theta}$ when considering the inter-cell interference for the UL transmission.

The overall interference $\hat{I}=\hat{I}_1+\hat{I}_2$, where $\hat{I}_1$ and $\hat{I}_2$ come from two independent HPPPs Φ^A and Φ^W. Moreover, the derivation of the Laplace transform is under the assumption that each co-channel cell is retained independently. Thus, we have

$$\begin{aligned}\mathcal{L}^{\hat{r}}_{\hat{I}}(s)&\triangleq\mathbb{E}_{\hat{I}}\left[\exp(-s\hat{I})\right]\\&=\mathbb{E}_{\hat{I}_1,\hat{I}_2}\left[\exp\left(-s(\hat{I}_1+\hat{I}_2)\right)\right]=\mathcal{L}^{\hat{r}}_{\hat{I}_1}(s)\cdot\mathcal{L}^{\hat{r}}_{\hat{I}_2}(s).\end{aligned} \tag{36}$$

As presented in **Lemma 2**, in the heterogeneous MHCP, we have to consider the different types of the considered typical cell. If the typical cell is an ID-CSMA cell, the Laplace transform of the aggregate interference for its DL and UL, $\hat{I}_d^A$ and $\hat{I}_u^A$, respectively, can be formulated as

$$\begin{aligned}&\mathcal{L}^{\hat{r}}_{\hat{I}_d^A}(s)\\&=\mathcal{L}^{\hat{r}}_{\hat{I}_1}\left(s,\hat{\kappa}=\kappa_{AA}\right)\cdot\mathcal{L}^{\hat{r}}_{\hat{I}_2}\left(s,\hat{\kappa}=\kappa_{AW}\right)|_{g=l},\\&\mathcal{L}^{\hat{r}}_{\hat{I}_u^A}(s)\\&=\mathcal{L}^{\hat{r}}_{\hat{I}_1}\left(s,\hat{\kappa}=\kappa_{AA}\right)\cdot\mathcal{L}^{\hat{r}}_{\hat{I}_2}\left(s,\hat{\kappa}=\kappa_{AW}\right)|_{g=\sqrt{\hat{r}^2+l^2-2\hat{r}l\cos\theta}}.\end{aligned} \tag{37}$$

Note that, in the above expressions, the different cases of $\hat{\kappa}(\cdot)$ in Eq. (34) are substituted in according to the interference source, such as $\hat{\kappa}=\kappa_{AA}$.

In contrast, if the typical cell is a Wi-Fi cell, the Laplace transform of the aggregate interference for its DL and UL, $\hat{I}_d^W$

and $\hat{I}_u^W$, respectively, can be formulated as

$$\begin{aligned}&\mathcal{L}_{\hat{I}_d^W}^{\hat{r}}(s)\\&=\mathcal{L}_{\hat{I}_1}^{\hat{r}}\left(s,\hat{\kappa}=\kappa_{WA}\right)\cdot\mathcal{L}_{\hat{I}_2}^{\hat{r}}\left(s,\hat{\kappa}=\kappa_{WW}\right)|_{g=l},\\&\mathcal{L}_{\hat{I}_u^W}^{\hat{r}}(s)\\&=\mathcal{L}_{\hat{I}_1}^{\hat{r}}\left(s,\hat{\kappa}=\kappa_{WA}\right)\cdot\mathcal{L}_{\hat{I}_2}^{\hat{r}}\left(s,\hat{\kappa}=\kappa_{WW}\right)|_{g=\sqrt{\hat{r}^2+l^2-2\hat{r}l\cos\theta}}.\end{aligned} \tag{38}$$

D. Average Ergodic Rate

1) For a Typical ID-CSMA Cell: With the distribution of serving distance $\hat{r}$ in Eq. (30), the Laplace transform of the aggregate interference obtained above for a typical ID-CSMA cell in (37), and the equal time-split for its TDD transmission model, we can formulate the average ergodic rate of the DL and UL as

$$\begin{aligned}\hat{\rho}_d^A=&\frac{1}{2}\int_0^\infty 2\pi\left(\lambda_s^A+\lambda_s^W\right)\hat{r}\exp\left(-\pi\left(\lambda_s^W+\lambda_s^A\right)\hat{r}^2\right)\\&\int_0^\infty\exp\left(-\frac{\hat{r}^{\alpha^W}\sigma^2}{P_s^AL_0^W}\left(e^t-1\right)\right)\mathcal{L}_{\hat{I}_d^A}^{\hat{r}}\left(\frac{\hat{r}^{\alpha^W}}{P_s^AL_0^W}\left(e^t-1\right)\right)\mathrm{d}t\mathrm{d}\hat{r}\end{aligned} \tag{39}$$

and

$$\begin{aligned}\hat{\rho}_u^A=&\frac{1}{2}\int_0^\infty 2\pi\left(\lambda_s^A+\lambda_s^W\right)\hat{r}\exp\left(-\pi\left(\lambda_s^W+\lambda_s^A\right)\hat{r}^2\right)\\&\int_0^\infty\exp\left(-\frac{\hat{r}^{\alpha^W}\sigma^2}{P_u^AL_0^W}\left(e^t-1\right)\right)\mathcal{L}_{\hat{I}_u^A}^{\hat{r}}\left(\frac{\hat{r}^{\alpha^W}}{P_u^AL_0^W}\left(e^t-1\right)\right)\mathrm{d}t\mathrm{d}\hat{r}.\end{aligned} \tag{40}$$

Note that, since the ID-CSMA cells operate in unlicensed spectrum, the path-loss exponent α^W and the reference path-loss L_0^W for the unlicensed band are used here.

2) For a Typical Wi-Fi Cell: The average ergodic rate of the DL and UL for the typical Wi-Fi cell, $\hat{\rho}_d^W$ and $\hat{\rho}_u^W$, have similar formulations than $\hat{\rho}_d^A$ and $\hat{\rho}_u^A$. Compared with $\hat{\rho}_d^A$ and $\hat{\rho}_u^A$ obtained above, for $\hat{\rho}_d^W$ and $\hat{\rho}_u^W$: *1)* the transmission powers are P_s^W and P_u^W, *2)* the Laplace transforms of aggregate interference are $\mathcal{L}_{\hat{I}_d^W}^{\hat{r}}(\cdot)$ and $\mathcal{L}_{\hat{I}_u^W}^{\hat{r}}(\cdot)$, and *3)* the time fractions are $\mathbb{E}_{\hat{n}}\left[\xi(\hat{n})\right]$ and $\mathbb{E}_{\hat{n}}\left[\hat{n}\xi(\hat{n})\right]$, respectively.

E. Area System Throughput in the Unlicensed Band

Both ID-CSMA and Wi-Fi cells contribute to the AST in the unlicensed spectrum. Since ID-CSMA cells work in a similar way as LTE cells, its effective resource utilisation factors for DL and UL are η_d^L and η_u^L, respectively. And hence, the throughput in the typical transmitting ID-CSMA cell can be formulated as $\frac{B^W}{M}\left(\eta_d^L\hat{\rho}_d^A+\eta_u^L\hat{\rho}_u^A\right)$, while that in the typical transmitting Wi-Fi cell is given by $\frac{B^W}{M}\eta^W\left(\hat{\rho}_d^W+\hat{\rho}_u^W\right)$.

Denoted by $\widehat{\Pr}(\mathcal{T})$ the probability that the typical cell is granted transmission in a heterogeneous MHCP, and taking into consideration the intensities of active ID-CSMA and Wi-Fi cells, the overall AST in the unlicensed band in the coexisting architecture is given by

$$\begin{aligned}\widehat{AST}^W=&\hat{A}\lambda_s^W\cdot\widehat{\Pr}(\mathcal{T})\cdot\frac{B^W}{M}\eta^W\left(\hat{\rho}_d^W+\hat{\rho}_u^W\right)\\&+\hat{A}\lambda_s^A\cdot\widehat{\Pr}(\mathcal{T})\cdot\frac{B^W}{M}\left(\eta_d^L\hat{\rho}_d^A+\eta_u^L\hat{\rho}_u^A\right),\end{aligned} \tag{41}$$

where $\widehat{\Pr}(\mathcal{T})=\frac{1-\exp(-C')}{C'}$.

VI. Network Performance Analysis of the Boost Architecture

In the *Boost* architecture, LTE works in the licensed spectrum for the UL transmissions for all the UE, i.e., $\lambda_u=\lambda_u^L+\lambda_u^W$, and Wi-Fi works in the unlicensed spectrum for the DL transmissions for all the UE. Therefore, the network performance of the *Boost* architecture consists of two parts: *1)* the UL Performance of LTE and *2)* the DL performance of Wi-Fi. In the following subsections, we present the results for those two parts.

A. The UL Performance of the LTE in Boost

Since in *Boost* the intensity of BSs in the LTE system, λ_s^L, is the same as that in the traditional architecture, we have that the average ergodic rate of LTE UL in *Boost* equals to that in the traditional architecture, that is, $\bar{\rho}_u^L=\rho_u^L$.

However, because the whole LTE system now only serves UL transmissions, the bandwidth originally allocated to the DL can now be allocated to the UL. Therefore, we can get the UL AST of *Boost*, also the AST in the licensed band, denoted by $\overline{AST}^L$, as

$$\overline{AST}^L=\lambda_s^LB^L\eta_u^L\rho_u^L. \tag{42}$$

B. The DL Performance of the Wi-Fi in Boost

1) Transmissions Inside a Wi-Fi cell: Since in *Boost* the Wi-Fi APs have to serve the DL transmission for all the UEs in the network with intensity λ_u, the PMF of the UE number in each cell in *Boost*, denoted by $\bar{n}$, can be represented as $\bar{n}\sim\mathrm{NB}\left(K,\frac{\lambda_u}{\lambda_u+K\lambda_s^W}\right)$. Therefore, the probability of activation of a Wi-Fi cell in *Boost*, which is equal to the probability that there is at least one UE in the cell, is given by

$$\bar{A}=1-\left(1-\frac{\lambda_u}{\lambda_u+K\lambda_s^W}\right)^K. \tag{43}$$

In *Boost*, the AP is the only transmitter inside a Wi-Fi cell. Since there is no contention inside a cell (no UL traffic), the transmission probability that an AP obtains inside the cell under CSMA/CA protocol equals to $\xi(0)$.

2) Simultaneous Transmission of Cells: The inter-cell channel contention in the *Boost* architecture is similar with that in the traditional architecture. And hence, a modified MHCP $\bar{\phi}_{x_0}^M$ can be used to model the positions of Wi-Fi cells in *Boost* that win the chance to transmit in a time instance. Compared with that in the traditional architecture, $\bar{\phi}_{x_0}^M$ is retained from the HPPP of the active co-channel Wi-Fi cells with intensity $\frac{\bar{A}}{M}\lambda_s^W$. Also, since the AP is the only transmitter inside a Wi-Fi cell, the expected transmission power in each cell equals to the transmission power of the AP, P_s^W.

Substituting the intensity $\frac{\bar{A}}{M}\lambda_s^W$ and the expected transmission power P_s^W, the probability that the typical cell is granted transmission in the MHCP $\bar{\phi}_{x_0}^M$, can be given by

$$\overline{\Pr}(\mathcal{T}) = \frac{1-\exp\left(-\frac{\bar{A}}{M}\lambda_s^W \bar{c}\right)}{\frac{\bar{A}}{M}\lambda_s^W \bar{c}}, \tag{44}$$

where $\bar{c} = 2\pi\int_0^\infty \exp\left(-\frac{\Gamma}{P_s^W L_0^W y^{-\alpha^W}}\right) y\mathrm{d}y$.

Since the intensity of active Wi-Fi cells in *Boost* is $\bar{A}\lambda_s^W$, the intensity of cells (i.e., APs in Boost) that grab the chance to transmit in a time instance can be formulated as $\bar{A}\lambda_s^W\overline{\Pr}(\mathcal{T})$. Based on the formulation of $\bar{A}$ in Eq. (41), we have $\lim_{\lambda_s^W\to\infty}\bar{A}\lambda_s^W = \lambda_u$, which leads to

$$\lim_{\lambda_s^W\to\infty}\bar{A}\lambda_s^W\overline{\Pr}(\mathcal{T}) = \frac{M}{\bar{c}}\left(1-\exp\left(-\frac{\bar{c}}{M}\lambda_u\right)\right). \tag{45}$$

From (45), we can draw the following remarks.

Remark 1. *In Boost, given M, λ_u, Γ and P_s^W, the intensity of the simultaneously transmitting APs monotonically increases with the intensity of the deployed APs λ_s^W, and converges to a constant when λ_s^W is sufficiently large.*

Remark 2. *In Boost, given Γ and P_s^W, when λ_s^W and λ_u are both sufficiently large, the intensity of the simultaneously transmitting APs in each channel converges to a constant $\frac{1}{\bar{c}}$.*

3) Inter-Wi-Fi cell Interference: Let us denote by $\bar{\phi}_{x_0}^I$ the positions of interfering cells when the typical cell is transmitting. Because there is only DL transmissions in each Wi-Fi cell, the aggregated interference for the DL in the typical cell, $\bar{I}_d$, can be formulated as

$$\bar{I}_d \approx \sum_{x_i\in\bar{\phi}_{x_0}^I:\|x_i\|>r} \xi(0)P_s^W h_i L_0^W \|x_i\|^{-\alpha^W}. \tag{46}$$

Moreover, we can obtain the retained probability $\bar{\kappa}(\cdot)$ in *Boost* according to (17), (18) and (19) with the intensity of contending cells $\frac{\bar{A}}{M}\lambda_s^W$ and the expected transmission power $P_{ave}^W = P_s^W$. Hence, the Laplace transform of the aggregate interference $\bar{I}_d$ can be written as

$$\mathcal{L}_{\bar{I}_d}^r(s) = \exp\left(-\frac{\bar{A}\lambda_s^W}{M}\int_0^{2\pi}\int_r^\infty \bar{\kappa}\left(\sqrt{r^2+l^2-2rl\cos\theta}\right)\left(1-\frac{1}{\left(1+s\cdot\xi(0)P_s^W L_0^W l^{-\alpha^W}\right)}\right) l\mathrm{d}l\mathrm{d}\theta\right). \tag{47}$$

Based on the definition of the function $\bar{\kappa}(\cdot)$ and $\lim_{\lambda_s^W\to\infty}\bar{A}\lambda_s^W = \lambda_u$, we have

$$\lim_{\lambda_s^W\to\infty}\frac{\bar{A}\lambda_s^W}{M}\cdot\bar{\kappa}(z) = \left(1-\exp\left(\frac{-\Gamma}{P_s^W L_0^W z^{-\alpha^W}}\right)\right)\cdot\left(\frac{\exp\left(-\frac{\lambda_u}{M}\bar{c}\right)}{-\bar{c}} + \frac{1-\exp\left(-\frac{\lambda_u}{M}(\bar{b}(z)-\bar{c})\right)}{\frac{\lambda_u}{M}\bar{c}(\bar{b}(z)-\bar{c})} + \frac{1-\exp\left(-\frac{\lambda_u}{M}(\bar{b}(z)-\bar{c})\right)}{-\frac{\lambda_u}{M}(\bar{b}(z)-\bar{c})^2} + \frac{1}{\bar{b}(z)-\bar{c}}\right), \tag{48}$$

where

$$\bar{b}(z) = 2\bar{c} - \int_0^\infty\int_0^{2\pi}\exp\left(-\frac{\Gamma}{P_s^W L_0^W}\cdot\left(\tau^{\alpha^W}+\left(\tau^2+z^2-2\tau z\cos\omega\right)^{\alpha^W/2}\right)\right)\tau\mathrm{d}\omega\mathrm{d}\tau.$$

From Eq. (48), we can draw the following remarks.

Remark 3. *In Boost, given Γ, P_s^W, M and λ_u, the Laplace transform of the aggregate interference converges to a constant when λ_s^W is sufficiently large.*

Remark 4. *In Boost, given Γ, P_s^W, when λ_s^W and λ_u are both sufficiently large, the Laplace transform of the aggregate interference is independent of the channel number M and converges to a constant.*

4) The DL SINR Distribution of Wi-Fi in Boost: With the pdf of r, the distance between the typical UE and its serving AP, we can formulate the CCDF of DL SINR in *Boost* as

$$\begin{aligned}\Pr\left[\bar{\gamma}_d^W \geq \delta\right] &\triangleq \Pr\left[\frac{P_s^W h_0 L_0^W r^{-\alpha^W}}{\bar{I}_d+\sigma^2}\geq\delta\right]\\ &= \int_0^\infty \exp\left(-\frac{r^{\alpha^W}\delta\sigma^2}{P_s^W L_0^W}\right)2\pi\lambda_s^W r\exp(-\pi\lambda_s^W r^2)\\ &\exp\left(-\frac{\bar{A}\lambda_s^W}{M}\int_0^{2\pi}\int_r^\infty \bar{\kappa}\left(\sqrt{r^2+l^2-2rl\cos\theta}\right)\left(1-\frac{1}{\left(1+\xi(0)\delta r^{\alpha^W}l^{-\alpha^W}\right)}\right)l\mathrm{d}l\mathrm{d}\theta\right)\mathrm{d}r.\end{aligned} \tag{49}$$

5) The DL Average Ergodic Rate of Wi-Fi in Boost: Denoted by $\bar{\rho}_d^W$ the DL average ergodic rate of Wi-Fi in Boost, we can obtain that

$$\begin{aligned}\bar{\rho}_d^W &= \xi(0)\cdot\mathbb{E}_{\bar{\gamma}_d^W}\left[\ln(1+\bar{\gamma}_d^W)\right]\\ &= \xi(0)\cdot\int_0^\infty 2\pi\lambda_s^W r\exp\left(-\pi\lambda_s^W r^2\right)\cdot\\ &\int_0^\infty\exp\left(-\frac{r^{\alpha^W}\sigma^2}{P_s^W}(e^t-1)\right)\cdot\\ &\exp\left(-\frac{\bar{A}\lambda_s^W}{M}\int_0^{2\pi}\int_r^\infty\bar{\kappa}\left(\sqrt{r^2+l^2-2rl\cos\theta}\right)\left(1-\frac{1}{\left(1+\xi(0)r^{\alpha^W}l^{-\alpha^W}(e^t-1)\right)}\right)l\mathrm{d}l\mathrm{d}\theta\right)\mathrm{d}t\mathrm{d}r.\end{aligned} \tag{50}$$

6) AST of Wi-Fi in Boost: Based on the DL average ergodic rate $\bar{\rho}_d^W$ in (41), and considering the Wi-Fi efficiency η^W and the bandwidth of each channel, we can formulate the AST of Wi-Fi in the unlicensed band in the *Boost* architecture, $\overline{AST}^W$, as

$$\overline{AST}^W = \bar{A}\lambda_s^W\cdot\overline{\Pr}(\mathcal{T})\cdot\eta^W\frac{B^W}{M}\bar{\rho}_d^W. \tag{51}$$

VII. Simulations and Discussions

In this section, we present numerical and Monte-Carlo simulation results to compare the performance of the various architectures.

TABLE I
PARAMETERS USED IN SIMULATIONS

	LTE Systems	Wi-Fi/ID-CSMA Systems
Frequency	3.5GHz	5GHz
Bandwidth	100MHz	480MHz
Path Loss Model	$36.7\log_{10}(d)+22.7+26\log_{10}(f_c)$ d in km, f_c in GHz	
BS/AP Trans. Power	30dBm/10MHz	24dBm/20MHz
UE Trans. Power	23dBm/10MHz	18dBm/20MHz
Noise	-174 dBm/Hz	
BS/AP Noise Figure	5dB	5dB
UE Noise Figure	9dB	9dB

A. Scenarios and Parameters

In our Monte-Carlo simulations, the performance is averaged over 1000 network deployments, where in each case the BSs, the APs and the UEs are randomly distributed in an area of $2 \times 2\text{km}^2$ according to the HPPP assumption.

Specifically, in the traditional and *Boost* architectures, the intensities of the BSs and the APs are $50/\text{km}^2$ and $200/\text{km}^2$, respectively. The intensity of UEs is $2000/\text{km}^2$, among which $2/5$ of the UEs work in the licensed spectrum and the others in the unlicensed spectrum in the traditional architecture. For comparison, in the coexisting architecture, we set both the intensities of ID-CSMA BSs and Wi-Fi APs to $100/\text{km}^2$, keeping the total intensity the same as that in the other two architectures.

The DL and UL efficiency in LTE is respectively set to $11/14$ and $12/14$, considering the OFDM symbols used for control signalling [25]. The Wi-Fi efficiency is set to 0.9, which is an approximate value obtained from the typical values of related parameters in [12]. The unlicensed band in Wi-Fi is divided into $M = 12$ channels, and the carrier sensing threshold in the unlicensed spectrum is set to -82dBm per 20MHz. Other detail parameters used in our simulations are listed in Table I.

The time efficiency of CSMA protocol has been analysed in several previous works using Markov chains. According to [12] and based on the assumption of a saturated network, we approximately have $\xi(n) = a_1/(n+1+a_2) - a_3$ and $\vartheta(n) = b_1 - b_2 * \exp(-b_3 * (n+1))$. The values of a_1, a_2, a_3 and b_1, b_2, b_3 depend on the detail parameters adopted, for instance, the window size and the maximum back-off stage. The verification of these two functions is relegated to Appendix A.

B. The SINR Distributions

In Fig. 3, we present the DL SINR distributions for the investigated architectures with the parameters mentioned above. In the traditional architecture, DL transmissions include the LTE ones and the Wi-Fi ones, while *Boost*, all DL transmissions are Wi-Fi ones.

Firstly, from the figure we can see that in both architectures the simulation results about the DL SINR of Wi-Fi match with our numerical results. Since the performance analysis of LTE has been well established in other works, we do not perform such verification here. Secondly, we can also see that the DL SINR distribution of Wi-Fi, for both the traditional architecture and *Boost*, are better than that of LTE. The reasons behind this observation are: *1)* the Wi-Fi bandwidth is partitioned into $M = 12$ channels, and thus the intensity of co-channel cells, the number of interfering cells, is much less; *2)* the channel contention scheme in Wi-Fi mitigates the strength of the interference, which is less than the threshold Γ. Finally, comparing the DL performance in the traditional architecture (the mixed SINR distribution of Wi-Fi and LTE parts) with that in *Boost*, we can conclude that *Boost* improves the quality of DL transmissions.

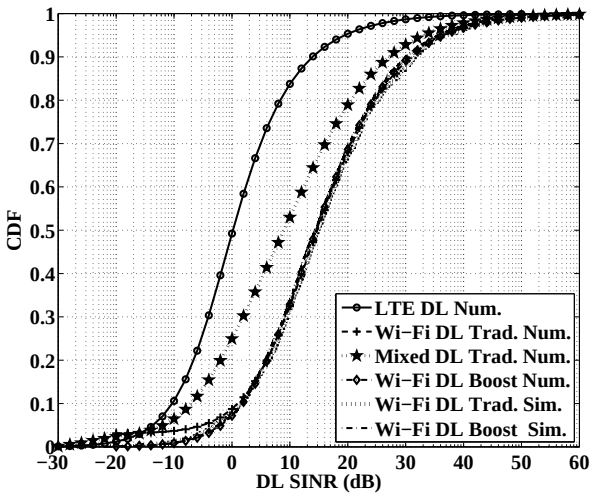

Fig. 3. DL SINR distributions in the traditional and *Boost* architectures.

Moreover, we can see that the DL SINR distributions of the Wi-Fi cells in these two architectures are very close to each other. This is due to the CSMA/CA contention protocol, and because the intensity of the co-channel Wi-Fi cells is rather small when $M = 12$. For the same reason, the DL SINR distributions of the ID-CSMA and Wi-Fi cells in the coexisting architecture are also very close to that of Wi-Fi cells in the traditional architecture. To show a clear figure, we omit those two curves in the coexisting architecture.

In Fig. 4, we plot the UL SINR distributions for the two architectures, assuming a fully loaded network where all UL resources are in use in all BSs and APs. Note that, in this figure, the UL power control factor used in LTE is 0.7. In the traditional architecture, UL transmissions include the LTE ones and the Wi-Fi ones, while in the Boost architecture, all UL transmissions are LTE ones. From the figure, we can see that the simulation results of the UL in the traditional Wi-Fi architecture match with the numerical results, which verifies the accuracy of our analysis. Moreover, compared with the DL SINR distributions in Fig. 3, the UL SINR distributions are not as good as the DL ones. The main reason is the smaller UL transmission powers adopted in both Wi-Fi and LTE, as well as the the power control scheme adopted in LTE aimed at saving transmit power at the UEs. Similarly to the DL case, the UL SINR in Wi-Fi is better than the UL SINR in LTE due to the less interference.

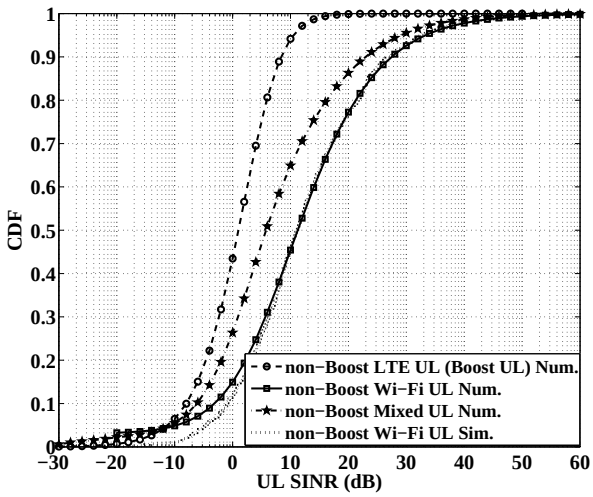

Fig. 4. UP SINR distributions in the traditional and *Boost* architectures.

C. The Performance for Boost

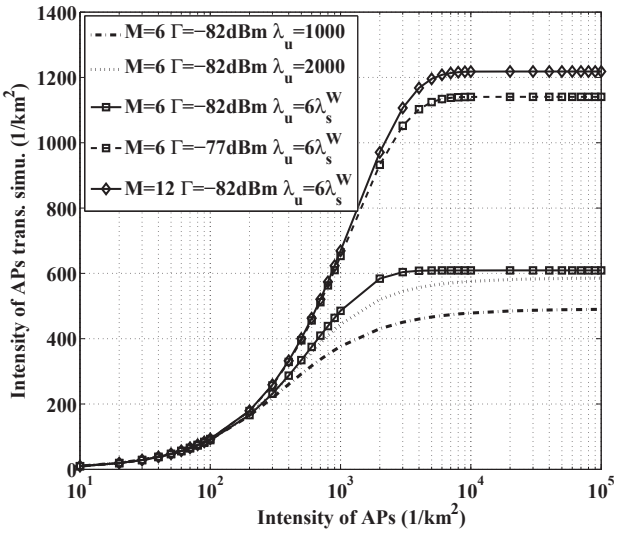

Fig. 5. The intensity of APs that can transmit simultaneously in *Boost*.

In Fig. 5, we show the intensity of APs that can transmit simultaneously compared with the intensity of the deployed APs, in the cases of different carrier sensing thresholds Γ and different channel numbers M. We can see that when the threshold Γ decreases from -77dBm to -82dBm (per 20MHz), the intensity of APs transmitting in one time instant decreases too. According to the CSMA protocol, a transmitter can only access the channel when all the co-channel signals received are less than this threshold. Therefore, a lower threshold implies a less chance for APs to access the medium, which leads to a lower intensity of the simultaneously transmitting APs. Moreover, from the figure, we can see that there are more APs transmitting in one time instant with a larger channel number M. Since channel contentions only occur among the co-channel APs, a larger M means that there are more orthogonal channels available for the APs. Therefore, more APs are transmitting simultaneously. Most importantly, we can also see that the intensity of the simultaneously transmitting APs increases with the intensity of the deployed APs λ_s^W. However, it reaches its limit when λ_s^W is sufficiently large. Moreover, when λ_u grows with λ_s^W to a sufficiently large value, the maximum intensity is proportional to the channel number M, which verifies Remark 2.

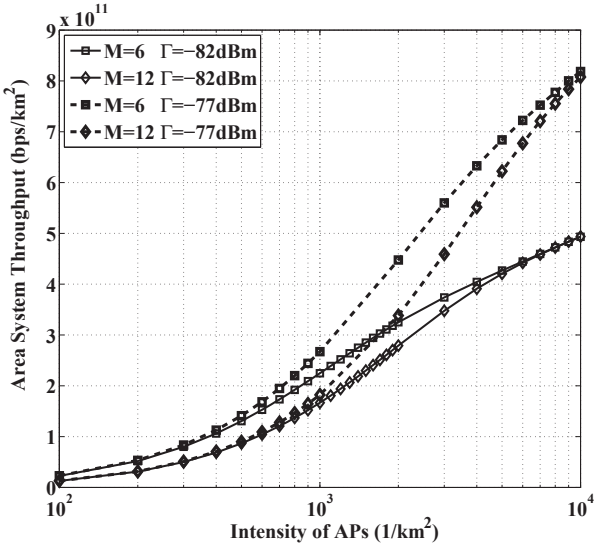

Fig. 6. The area system throughput in the unlicensed band with *Boost*.

In Fig. 6, we present the area system throughput (AST) in the unlicensed band for the *Boost* architecture. In this figure, $\lambda_u = 6\lambda_s^W$. Firstly, we can see that the AST increases with the intensity λ_s^W, the reasons are *1)* a larger λ_s^W implies a shorter distance between the serving AP and its UE and hence a stronger received signal, and *2)* as shown in Fig. 5, the intensity of APs that transmit simultaneously also increases with λ_s^W. Secondly, given λ_s^W, the AST with the threshold $\Gamma = -77$dBm is larger than that with $\Gamma = -82$dBm. As mentioned in the discussion for Fig. 5, the intensity of simultaneously transmitting APs increases with Γ, which contributes to the growth of the AST. Thirdly, a smaller channel number M generally leads to a larger AST, since the bandwidth for each channel, i.e., $\frac{B^W}{M}$, is larger. Moreover, this advantage starts disappearing when λ_s^W is sufficiently large.

D. The Comparison of the AST Performance for the Three Architectures

In Fig. 7, we compare the Wi-Fi performance in the unlicensed band for the three different architectures in terms of AST. In the traditional and coexisting architectures, the unlicensed band is used both for DL and UL transmissions, therefore, the area spectral efficiency consists of these two parts. In Boost, the unlicensed band is only used for DL transmissions. From the figure, we can see that in the traditional and coexisting architectures, the AST first increases with the UE-to-AP intensity ratio and then decreases with it. The reason for the increase part is the growth of the number of active

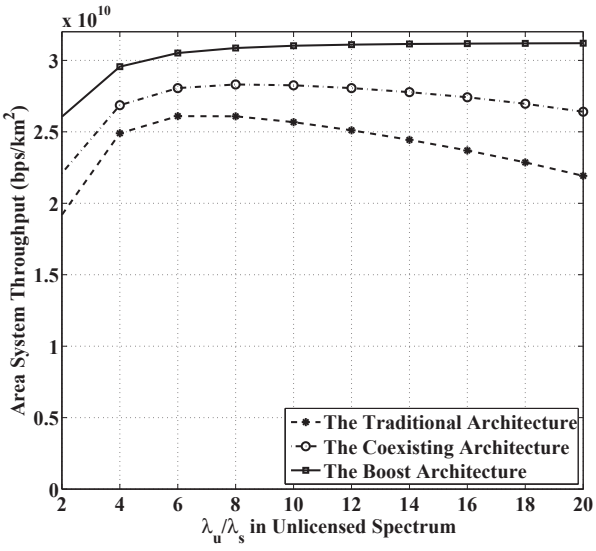

Fig. 7. The area system throughput in the unlicensed band with the three architectures.

cells, and thus the higher chance that UEs are closer to their serving BS. The reason for the decrease part is the growth of the number of collisions in Wi-Fi cells under the CSMA protocol, since more UEs are trying to content the channel.

From the figure, we can see that compared with the traditional architecture, *1)* the coexisting architecture has around 22% AST gain when the UE-to-AP intensity ratio increases to 20, and *2)* the *Boost* achieves around 45% AST gain.

The performance gain achieved be the coexisting architecture comes from the coordinated scheduling within the ID-CSMA cells. With the similar SINR performance, without contention inside the ID-CSMA cells, the spectral efficiency in ID-CSMA cells is higher than that in Wi-Fi cells. Wi-Fi cells suffer form such UL contention. In *Boost*, by avoiding the CSMA collisions inside all cells, the spectral efficiency is higher, and no performance degradation occurs when the UE intensity increases.

In Table II, we compare the AST in the three architectures when different maximum back-off stage is adopted in CSMA/CA protocol. Moreover, different UE-to-AP intensity ratios are involved to represent a normal-loaded (λ_u^W/λ_s^W =6) and a heavy-loaded scenario (λ_u^W/λ_s^W =16).

We can see that in all scenarios, the coexisting architecture outperforms the traditional architecture in terms of AST (licensed and unlicensed band with their DL and UL), while the system performance of the *Boost* is the best. In the normal-loaded scenarios and with respect to the traditional architecture, the performance gain of the coexisting architecture is around 5%, while that of *Boost* is around 15%. In heavy-loaded scenarios, the gains are 11% and 25%, respectively. As this results indicate the performance gains achieved by the coexisting architecture and the *Boost* in the heavy-loaded scenarios with $\lambda_u^W/\lambda_s^W = 16$ are more obvious than that in normal-loaded scenarios with $\lambda_u^W/\lambda_s^W = 6$. This is due to the larger collision avoidance. The performance gain of the *Boost* achieves 25% in the heavy-loaded scenarios, which indicates that *Boost* is very efficient in crowded areas like shopping malls, hospitals and so on.

VIII. Conclusions

In this paper, we first present a new framework to analyse the network performance of Wi-Fi. We jointly consider the DL and UL transmissions, the time efficiency degradation caused by the back-off scheme and collisions, as well as the interference and signal quality with spatial randomness. Then, using this framework, we analyse a network with coexisting ID-CSMA cells and Wi-Fi cells. Considering the impact of their different intra-cell schemes, a new heterogeneous MHCP model is used to analyse their inter-cell interference under CSMA. Moreover, the performance of *Boost* is also obtained using this framework. The simulation results verify our analysis, and show the performance of the coexisting and *Boost* architectures compared to that of the traditional network architecture. In normal-loaded scenarios, the gain in terms of AST achieved by the coexisting architecture are around 5%, and that of *Boost* are round 15%. In the heavy-loaded cases, the gains achieve 11% in the coexisting architecture and 25% in *Boost*. The coexisting architecture eliminates the channel contentions and collisions inside the ID-CSMA cells, while *Boost* eliminates them inside all cells operating in the unlicensed band. In other words, our study showed that the coexisting architecture cannot solve the low efficiency of the Wi-Fi network in the unlicensed band due to the access contention in the UL, especially when the UE number is large. *Boost* does not have this problem and thus performs better.

Appendix A
CSMA/CA in Wi-Fi networks

In a Wi-Fi network, when the AP or a UE wants to make a transmission, it senses the radio channel and performs a clear channel assessment check. If no transmissions are detected for a period of time, the transmission begins. Otherwise, the device draws an integer number uniformly at the contention window, and starts to count down. The counter is paused during periods when the channel is detected busy. When the counter reaches zero, the device proceeds with the transmission. If another device also transmits at the same time, then a collision occurs and the transmission possibly fails due to poor signal quality. When a transmission fails, a new random number is drawn and this process is repeated. The size of contention window doubles on each collision, namely, exponential back-off. After a successful transmission, the size of the contention window is set to its original value. The simplicity of CSMA/CA that causes Wi-Fi's poor performance in scenarios with a large number of devices.

From the analyze in [12], there are three states under the assumption of the CSMA/CA protocol: idle, transmission and collision, and the time spent on each state can be formulated as: $T_{\text{idle}} = (1-\tau)^{\hat{n}} \cdot \sigma$, $T_{\text{trans}} = \hat{n}\tau(1-\tau)^{\hat{n}-1} \cdot T_s$ and $T_{\text{colli}} = \left(1-(1-\tau)^{\hat{n}} - \hat{n}\tau(1-\tau)^{\hat{n}-1}\right) \cdot T_c$. Here $\hat{n} = n+1$ denotes the nodes' number including the AP, and τ is the probability that a node attempts transmission which is the resolution of a nonlinear equations obtained by Markov chain. Moreover, σ

TABLE II
COMPARISON OF AREA SYSTEM THROUGHPUT IN THE TRADITIONAL AND BOOST ARCHITECTURES

Network Architecture		Maximum Back-off Stage is 5		Maximum Back-off Stage is 3	
		$\lambda_u^W/\lambda_s^W=6$	$\lambda_u^W/\lambda_s^W=16$	$\lambda_u^W/\lambda_s^W=6$	$\lambda_u^W/\lambda_s^W=16$
Traditional Architecture (Gbps/km^2)	LTE DL	2.839			
	LTE UL	2.622			
	Wi-Fi DL	5.893	2.542	5.890	2.538
	Wi-Fi UL	20.202	21.153	20.182	21.097
	Total	31.556	29.156	31.533	29.096
Coexisting Architecture (Gbps/km^2)	LTE DL	2.839			
	LTE UL	2.622			
	Wi-Fi DL	2.9179	1.253	2.916	1.251
	Wi-Fi UL	10.002	10.428	9.992	10.400
	ID-CSMA DL	7.8384	8.086	7.834	8.073
	ID-CSMA UL	7.025	7.264	7.018	7.244
	Total	33.244	32.492	33.221	32.429
	Gain	5.35%	11.44%	5.35%	11.46%
Boost Architecture (Gbps/km^2)	LTE UL	5.244			
	Wi-Fi DL	31.025	31.201	31.025	31.201
	Total	36.269	36.445	36.269	36.446
	Gain	14.9%	25.0%	15.02%	25.26%

is the duration of an empty time-slot, T_s is the expected time taken for a successful transmission and T_c is the expected time taken for a collision.

The transmission probability that each node obtained, $\xi(n)=\frac{\tau(1-\tau)^{\hat{n}-1}T_s}{T_{\text{idle}}+T_{\text{trans}}+T_{\text{colli}}}$ and the collision probability $\vartheta(n)=\frac{T_{\text{colli}}}{T_{\text{idle}}+T_{\text{trans}}+T_{\text{colli}}}$. Since it is difficult to obtain exact expressions from them, we propose two approximate expressions: $\xi(n)=a_1/(n+1+a_2)-a_3$ and $\vartheta(n)=b_1-b_2*\exp\left(-b_3*(n+1)\right)$. Using the typical parameters adopted in 802.11, Fig. 8 and 9 compare our approximate expressions and the analytical results obtained in [12].

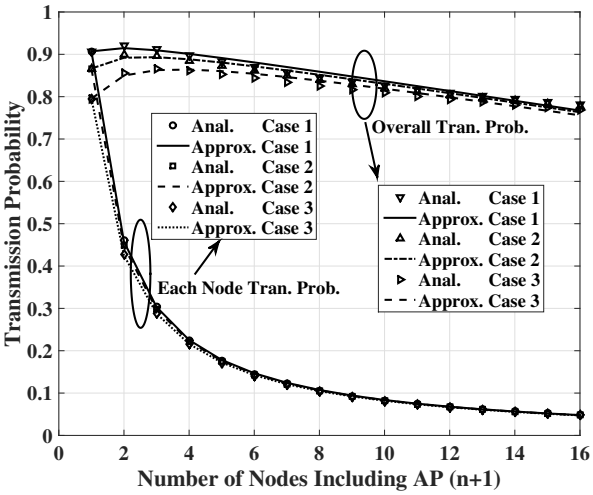

Fig. 8. Comparison of the analytical result and fitting curve.

Fig. 8 shows the results about the transmission probability for each node, $\xi(n)$, and the overall transmission probability, $(n+1)\xi(n)$. In "Case 1", the basic contention window size is 32, the the maximum back-off stage is 5, the duration of an empty time-slot $\sigma=20\mu$s, the expect time taken for a successful transmission $T_s=3000\mu$s, and the expected time taken for a collision T_c is assumed to be equal to T_s as in [13]. Compared to "Case 1", $T_s=2000\mu$s in "Case 2", while $\sigma=50\mu$s in "Case 3". The curves show a good match by adopting the approximate expression $\xi(n)$.

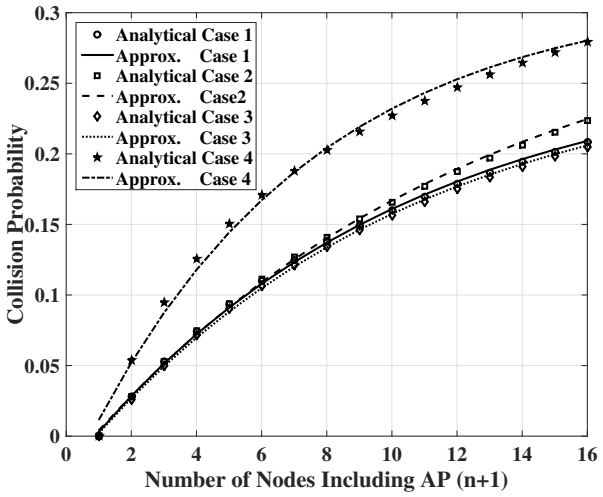

Fig. 9. Comparison of the analytical result and fitting curve.

Fig. 9 shows the collision probability $\vartheta(n)$ when the parameters are set to different values. "Case 1" in Fig. 9 adopts the same values with "Case 1" in Fig. 8. Then each other case changes the value of one parameter compared to "Case 1". In detail, "Case 2" changes the maximum back-off stage to 3, "Case 3" uses $\sigma=50\mu$s, and "Case 4" sets the basic contention window size as 16. We can see the good match in all cases with the approximate expression.

APPENDIX B
PROOF OF $\kappa(z)$

Given the typical cell $\mathcal{V}(x_0)$ is transmitting, the probability that the co-channel cell $\mathcal{V}(x_i)$ is an interfering cell equals to $\Pr\left[x_i\in\phi_{x_0}^M \mid x_0\in\phi_{x_0}^M\right]=\Pr\left[x_0\in\phi_{x_0}^M, x_i\in\phi_{x_0}^M\right]/\Pr\left[x_0\in\phi_{x_0}^M\right]$.

Assuming that the mark of x_0 is $m(x_0)=u$, based on the definition of the MHCP, x_0 is retained when all the point with

a smaller mark are outside its contention domain. Denoted by $\mathcal{N}(x_j, x_0)$ the event that x_j is outside the contention domain of x_0, i.e., x_0 dose not detect x_j, we have

$$\Pr\left[x_0 \in \phi_{x_0}^M\right] = \Pr\left[\forall x_j \in \phi_{x_0}, m(x_j) < u, \mathcal{N}(x_j, x_0)\right]. \tag{52}$$

Let us focus on the joint probability. Suppose that the mark of x_i is $m(x_i) = t$. When $t < u$, i.e., x_0 with a larger mark, x_0 and x_i are both retained if 1) x_0 does not detect x_i, and 2) both of them do not detect any point with mark less than t, and 3) x_0 does not detect any point with mark between t and u. Hence we have

$$\begin{aligned}\Pi_1 \triangleq& \Pr\left[x_0 \in \phi_{x_0}^M, x_i \in \phi_{x_0}^M \mid m(x_0) = u, m(x_i) = t, t < u\right] \\ =& \Pr\left[\mathcal{N}(x_i, x_0)\right] \\ &\cdot \Pr\left[\forall x_j \in \phi_{x_0}, m(x_j) < t, \mathcal{N}(x_j, x_0), \mathcal{N}(x_j, x_i)\right] \\ &\cdot \Pr\left[\forall x_j \in \phi_{x_0}, t < m(x_j) < u, \mathcal{N}(x_j, x_0)\right]\end{aligned}$$

Note that, $\mathcal{N}(y, x)$ denotes the event that $\mathcal{V}(x)$ dose not detect $\mathcal{V}(y)$.

When $t > u$, x_i has a larger mark. And hence, x_0 and x_i are both retained if 1) x_i does not detect x_0, and 2) both of them do not detect any point with mark less than u, and 3) x_i does not detect any point with mark between t and u. That is,

$$\begin{aligned}\Pi_2 \triangleq& \Pr\left[x_0 \in \phi_{x_0}^M, x_i \in \phi_{x_0}^M \mid m(x_0) = u, m(x_i) = t, t > u\right] \\ =& \Pr\left[\mathcal{N}(x_0, x_i)\right] \\ &\cdot \Pr\left[\forall x_j \in \phi_{x_0}, m(x_j) < u, \mathcal{N}(x_j, x_0), \mathcal{N}(x_j, x_i)\right] \\ &\cdot \Pr\left[\forall x_j \in \phi_{x_0}, u < m(x_j) < t, \mathcal{N}(x_j, x_i)\right]\end{aligned}$$

Then, based on the two parts of the joint probability, and Eq. (52), we have

$$\begin{aligned}&\Pr\left[x_i \in \phi_{x_0}^M \mid x_0 \in \phi_{x_0}^M\right] \\ &\quad= \int_0^1 \frac{\int_0^u \Pi_1 \mathrm{d}t + \int_u^1 \Pi_2 \mathrm{d}t}{\Pr\left[\forall x_j \in \phi_{x_0}, m(x_j) < u, \mathcal{N}(x_j, x_0)\right]} \mathrm{d}u.\end{aligned} \tag{53}$$

Since ϕ_{x_0} is an HPPP with intensity $\lambda = \frac{A}{M}\lambda_s^W$, according to [16], we have

$$\begin{aligned}&\Pr\left[\forall x_j \in \phi_{x_0}, k_1 < m(x_j) < k_2, \mathcal{N}(x_j, x)\right] \\ &\qquad= \exp\left(-\lambda(k_2 - k_1)c\right),\end{aligned} \tag{54}$$

where $c = \int_{\mathbb{R}^2} \left(1 - \Pr\left[\mathcal{N}\left(x_j, x\right)\right]\right) \mathrm{d}x_j$, and

$$\begin{aligned}&\Pr\left[\forall x_j \in \phi_{x_0}, m(x_j) < k, \mathcal{N}(x_j, x_0), \mathcal{N}(x_j, x_i)\right] \\ &\qquad= \exp\left(-k\lambda b(z)\right),\end{aligned} \tag{55}$$

where $b(z) = \int_{\mathbb{R}^2} \left(1 - \Pr\left[\mathcal{N}\left(x_j, x_0\right), \mathcal{N}\left(x_j, x_i\right)\right]\right) \mathrm{d}x_j$ and $z = \|x_i - x_0\|$. Also, following the definition in (14), we have $\Pr\left[\mathcal{N}(x_j, x)\right] = P\left(\mathcal{V}(x_j), \mathcal{V}(x)\right) \leq \Gamma$. Then, substituting all the expressions in (53), we finish the proof.

Note that, in heterogeneous MHCP, an interfering cell can be an ID-CSMA or a Wi-Fi cell. That is, we have to consider two different cases for x_j involved in (54) and (55), since the expected transmission powers and the intensities for ID-CSMA and Wi-Fi cells are different.

APPENDIX C
PROOF OF LAPLACE TRANSFORM $\mathcal{L}_{I_d}^r$ AND $\mathcal{L}_{I_u}^r$

Since the formulation of I_d and I_u in (15) and (16) have similar formulations, we focus on $\mathcal{L}_{I_d}^r$ first. Since $\mathcal{L}_{I_d}^r(s) = \mathbb{E}_{I_d}\left[\exp\left(-sI_d\right)\right]$, we can derive it as (56), shown in the top of the next page.

Note that, in (56), (a) uses $g \triangleq \|x_0\|$, (b) uses the distribution of h_i, $h_{i,j}$ and $h_{i,i}$, as well as their independence, (c) uses the assumption that the co-channel cells in ϕ_{x_0} are retained independently according to the probability $\kappa(\cdot)$.

Since $r \triangleq \|x_0\|$, using polar coordinate (l, θ) to represent the point x_i, we have the distance $\|x_i - x_0\| = \sqrt{(r^2 + l^2 - 2rl\cos\theta)}$. With the constraint $\|x_i\| > r$ and the PMF of n_i, we complete the proof.

REFERENCES

[1] S. Sesia, I. Toufik, and M. Baker, Eds., *The UMTS Long Term Evolution: From Theory to Practice*, 2nd ed. Wiley & Sons, Feb. 2009.

[2] E. Perahia and R. Stacey, *Next Generation Wireless LANs: 802.11n and 802.11ac*, 2nd ed. Cambridge University Press, Jun. 2013.

[3] S. Sagari, S. Baysting, D. Saha, I. Seskar, W. Trappe, and D. Raychaudhuri, "Coordinated dynamic spectrum management of LTE-U and Wi-Fi networks," in *2015 IEEE International Symposium on Dynamic Spectrum Access Networks (DySPAN)*, Sept 2015, pp. 209–220.

[4] J. Jeon, Q. C. Li, H. Niu, A. Papathanassiou, and G. Wu, "LTE in the unlicensed spectrum: A novel coexistence analysis with WLAN systems," in *2014 IEEE Global Communications Conference*, Dec 2014, pp. 3459–3464.

[5] 3GPP, "Feasibility Study on Licensed-Assisted Access to Unlicensed Spectrum," 3GPP TR 36.889 v.13.0.0, Jul. 2015.

[6] 3GPP, "Evolved Universal Terrestial Radio Access (E-UTRA) and Evolved Universal Terrestial Radio Access Network (E-UTRAN); Overall description; Stage 2," 3GPP TS 36.300 v.13.3.0, Apr. 2016.

[7] 3GPP, "Evolved Universal Terrestrial Radio Access (E-UTRA) Radio Resource Control (RRC) Protocol specification," 3GPP TS 36.331 v.13.2.0, Jun. 2016.

[8] 3GPP, "LTE/WLAN Radio Level Integration Using IPsec Tunnel (LWIP) encapsulation," 3GPP TS 36.361 v.13.0.0, Apr. 2016.

[9] J. Andrews, F. Baccelli, and R. Ganti, "A Tractable Approach to Coverage and Rate in Cellular Networks," *IEEE Transactions on Communications*, vol. 59, no. 11, pp. 3122–3134, Nov. 2011.

[10] T. Novlan, H. Dhillon, and J. Andrews, "Analytical Modeling of Uplink Cellular Networks," *IEEE Transactions on Wireless Communications*, vol. 12, no. 6, pp. 2669–2679, June 2013.

[11] T. Ding, M. Ding, G. Mao, Z. Lin, D. Lpez-Prez, and A. Zomaya, "Uplink Performance Analysis of Dense Cellular Networks with LoS and NLoS Transmissions," *arXiv preprint arXiv:1609.07837*, Sep. 2016.

[12] G. Bianchi, "Performance analysis of the IEEE 802.11 distributed coordination function," *IEEE Journal on Selected Areas in Communications*, vol. 18, no. 3, pp. 535–547, March 2000.

[13] D. Malone, K. Duffy, and D. Leith, "Modeling the 802.11 Distributed Coordination Function in Nonsaturated Heterogeneous Conditions," *IEEE/ACM Transactions on Networking*, vol. 15, no. 1, pp. 159–172, Feb. 2007.

[14] O. Tickoo and B. Sikdar, "Modeling Queueing and Channel Access Delay in Unsaturated IEEE 802.11 Random Access MAC Based Wireless Networks," *IEEE/ACM Transactions on Networking*, no. 4, pp. 878–891, Aug.

[15] R. P. Liu, G. J. Sutton, and I. B. Collings, "A New Queueing Model for QoS Analysis of IEEE 802.11 DCF with Finite Buffer and Load," *IEEE Transactions on Wireless Communications*, vol. 9, no. 8, pp. 2664–2675, August 2010.

[16] H. Q. Nguyen, F. Baccelli, and D. Kofman, "A Stochastic Geometry Analysis of Dense IEEE 802.11 Networks," in *INFOCOM 2007. 26th IEEE International Conference on Computer Communications. IEEE*, May 2007, pp. 1199–1207.

[17] Y. Li, F. Baccelli, J. G. Andrews, T. D. Novlan, and J. Zhang, "Modeling and Analyzing the Coexistence of Wi-Fi and LTE in Unlicensed Spectrum," *arXiv preprint arXiv:1510.01392*, Dec 2015.

$$
\begin{aligned}
&\mathbb{E}_{I_d}\left[\exp\left(-s\left(\sum_{x_i\in\phi^I_{x_0}} L_0^W\|x_i\|^{-\alpha^W}\left(\xi(n_i)P_s^W h_i+\sum_{j=1}^{n_i}\xi(n_i)P_u^W h_{i,j}+\vartheta(n_i)2\frac{n_iP_u^W+P_s^W}{n_i+1}h_{i,i}\right)\right)\right)\right]\\
&\overset{(a)}{=}\mathbb{E}_{x_i,n_i,h_i,h_{i,j},h_{i,i}}\left[\prod_{x_i}\left(\exp\left(-sL_0^W g^{-\alpha^W}\xi(n_i)P_s^W h_i\right)\exp\left(-sL_0^W g^{-\alpha^W}\vartheta(n_i)2\frac{n_iP_u^W+P_s^W}{n_i+1}h_{i,i}\right)\right.\right.\\
&\left.\left.\prod_{j=1}^{n_i}\exp\left(-sL_0^W g^{-\alpha^W}\xi(n_i)P_u^W h_{i,j}\right)\right)\right]\\
&\overset{(b)}{=}\mathbb{E}_{x_i,n_i}\left[\prod_{x_i\in\phi^a_{x_0}}\left(\frac{1}{\left(1+s\xi(n_i)P_s^W L_0^W g^{-\alpha^W}\right)}\cdot\frac{1}{\left(1+s\vartheta(n_i)\hat{P}^{col}_{x_i}L_0^W g^{-\alpha^W}\right)}\cdot\left(\frac{1}{1+s\xi(n_i)P_u^W L_0^W g^{-\alpha^W}}\right)^{n_i}\right)\right]\\
&\overset{(c)}{\approx}\mathbb{E}_{n_i}\left[\exp\left(-\frac{A\lambda_s^W}{M}\int_{\mathbb{R}^2}\kappa\left(\|x_i-x_0\|\right)\right.\right.\\
&\left.\left.\left(1-\frac{1}{1+s\xi(n_i)P_s^W L_0^W g^{-\alpha^W}}\cdot\frac{1}{1+s\vartheta(n_i)\hat{P}^{col}_{x_i}L_0^W g^{-\alpha^W}}\cdot\frac{1}{\left(1+s\xi(n_i)P_u^W L_0^W g^{-\alpha^W}\right)^{n_i}}\right)\mathrm{d}x_i\right)\right].
\end{aligned}
\tag{56}
$$

[18] J. Ling, S. Kanugovi, S. Vasudevan, and A. K. Pramod, "Enhanced Capacity & Coverage by Wi-Fi LTE Integration," *IEEE Comm. Mag.*, vol. 53, no. 3, pp. 165–171, Mar. 2014.

[19] Nokia. (2015, Mar.) Wireless Unified Networks. [Online]. Available: https://networks.nokia.com/press/2015/alcatel-lucent-combines-best-wi-fir-and-lte-enhance-mobile-performance-and-offer-consistent-high

[20] B. Yu, L. Yang, H. Ishii, and S. Mukherjee, "Dynamic TDD Support in Macrocell-Assisted Small Cell Architecture," *IEEE Journal on Selected Areas in Communications*, vol. 33, no. 6, pp. 1201–1213, June 2015.

[21] S. Lee and K. Huang, "Coverage and Economy of Cellular Networks with Many Base Stations," *IEEE Communications Letters*, vol. 16, no. 7, pp. 1038–1040, July 2012.

[22] M. Haenggi, *Stochastic Geometry for Wireless Networks*. Cambridge University Press, 2012.

[23] M. Iwamura, K. Etemad, M. h. Fong, R. Nory, and R. Love, "Carrier aggregation framework in 3GPP LTE-advanced [WiMAX/LTE Update]," *IEEE Communications Magazine*, vol. 48, no. 8, pp. 60–67, August 2010.

[24] H. S. Jo, Y. J. Sang, P. Xia, and J. G. Andrews, "Heterogeneous Cellular Networks with Flexible Cell Association: A Comprehensive Downlink SINR Analysis," *IEEE Transactions on Wireless Communications*, vol. 11, no. 10, pp. 3484–3495, October 2012.

[25] 3GPP, "Evolved Universal Terrestial Radio Access; Further Enhancements for E-UTRA physical layer aspects," 3GPP TR 36.872 v.9.0.0, Mar. 2010.

Youjia Chen received the B.S. and M.S degrees in communication engineering from Nanjing University, Nanjing, China, in 2005 and 2008, respectively. From 2008-2009, she worked in Alcatel Lucent Shanghai Bell. From Aug. 2009 until now, she works at the College of Photonic and Electrical Engineering, Fujian Normal University, China. She is currently pursuing the Ph.D. degree in wireless engineering at The University of Sydney, Australia. Her current research interests include resource management, load balancing, and caching strategy in heterogeneous cellular networks.

Ming Ding (M'12) received the B.S. and M.S. degrees (with first class Hons.) in electronics engineering from Shanghai Jiao Tong University (SJTU), Shanghai, China, and the Doctor of Philosophy (Ph.D.) degree in signal and information processing from SJTU, in 2004, 2007, and 2011, respectively. From September 2007 to September 2011, he pursued the Ph.D. degree at SJTU while at the same time working as a Researcher/Senior Researcher Sharp Laboratories of China (SLC). After achieving the Ph.D. degree, he continued working with SLC as a Senior Researcher/Principal Researcher until September 2014, when he joined National Information and Communications Technology Australia (NICTA). In September 2015, Commonwealth Scientific and Industrial Research Organization (CSIRO) and NICTA joined forces to create Data61, where he continued as a Senior Research Scientist in this new R&D centre located in Sydney, N.S.W., Australia. He has authored about 40 papers in IEEE journals and conferences, all in recognized venues, and about 20 3GPP standardization contributions, as well as a Springer book Multi-point Cooperative Communication Systems: Theory and Applications. Also, as the first inventor, he holds fifteen CN, seven JP, three US, two KR patents and co-authored another 100+ patent applications on 4G/5G technologies. He is or has been Guest Editor/Co-Chair/TPC member of several IEEE top-tier journals/conferences, e.g., the IEEE Journal on Selected Areas in Communications, the IEEE Communications Magazine, and the IEEE Globecom Workshops. For his inventions and publications, he was the recipient of the President's Award of SLC in 2012, and served as one of the key members in the 4G/5G standardization team when it was awarded in 2014 as Sharp Company Best Team: LTE 1014 Standardization Patent Portfolio.

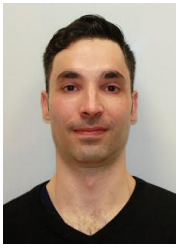

David López-Pérez (M'12) is a Member of Technical Staff at Nokia Bell Laboratories, and his main research interests are in HetNets, small cells, massive MIMO, interference and mobility management as well as network optimization and simulation. Prior to this, David earned his PhD in Wireless Networking from the University of Bedfordshire, UK in Apr. '11, and obtained his BSc and MSc degrees in Telecommunication from the Miguel Hernandez University, Spain in Sept. '03 & Sept. '06, respectively. David was Research Associate at King's College London, UK from Aug. '10 to Dec. '11, carrying post-doctoral studies, and was with VODAFONE, Spain from Feb. '05 to Feb. '06, working in the area of network planning and optimization. For his publications and patent contributions, David is a recipient of both the Bell Labs Alcatel-Lucent Award of Excellence (2013) and Certificate of Outstanding Achievement (2013, 2014, 2015). He was also finalist for the Scientist of the Year prize in The Irish Laboratory Awards (2013, 2015). David has also been awarded as PhD Marie-Curie Fellow in 2007 and Exemplary Reviewer for IEEE Communications Letters in 2011. David is author of the book "Heterogeneous Cellular Networks: Theory, Simulation and Deployment" Cambridge University Press, 2012. Moreover, he has published more than 90 book chapters, journal and conference papers, all in recognized venues, and filed more than 30patents applications. David is or has been guest editor of a number of journals, e.g., IEEE JSAC, IEEE Comm. Mag., and TPC member of top tier conferences, e.g., IEEE Globecom and IEEE ICC.

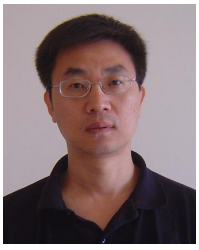

Zihuai Lin (S'98-M'06-SM'10) received the Ph.D. degree in Electrical Engineering from Chalmers University of Technology, Sweden, in 2006. Prior to this he has held positions at Ericsson Research, Stockholm, Sweden. Following Ph.D. graduation, he worked as a Research Associate Professor at Aalborg University, Denmark and currently at the School of Electrical and Information Engineering, the University of Sydney, Australia. His research interests include source/channel/network coding, coded modulation, MIMO, OFDMA, SC-FDMA, radio resource management, cooperative communications, small-cell networks, 5G cellular systems, etc.

Guoqiang Mao (S'98-M'02-SM'08) received PhD in telecommunications engineering in 2002 from Edith Cowan University. He was with the School of Electrical and Information Engineering, the University of Sydney between 2002 and 2014. He joined the University of Technology Sydney in February 2014 as Professor of Wireless Networking and Director of Center for Real-time Information Networks. The Center is among the largest university research centers in Australia in the field of wireless communications and networking. He has published about 200 papers in international conferences and journals, which have been cited more than 4000 times. He is an editor of the IEEE Transactions on Wireless Communications (since 2014), IEEE Transactions on Vehicular Technology (since 2010) and received Top Editor award for outstanding contributions to the IEEE Transactions on Vehicular Technology in 2011, 2014 and 2015. He is a co-chair of IEEE Intelligent Transport Systems Society Technical Committee on Communication Networks. He has served as a chair, co-chair and TPC member in a large number of international conferences. His research interest includes intelligent transport systems, applied graph theory and its applications in telecommunications, Internet of Things, wireless sensor networks, wireless localization techniques and network performance analysis.